

Predictive Coding Networks and Inference Learning: Tutorial and Survey

BJÖRN VAN ZWOL, RO JEFFERSON, and EGON L. VAN DEN BROEK, Utrecht University, The Netherlands

Recent years have witnessed a growing call for renewed emphasis on neuroscience-inspired approaches in artificial intelligence research, under the banner of *NeuroAI*. A prime example of this is predictive coding networks (PCNs), based on the neuroscientific framework of predictive coding. This framework views the brain as a hierarchical Bayesian inference model that minimizes prediction errors through feedback connections. Unlike traditional neural networks trained with backpropagation (BP), PCNs utilize inference learning (IL), a more biologically plausible algorithm that explains patterns of neural activity that BP cannot. Historically, IL has been more computationally intensive, but recent advancements have demonstrated that it can achieve higher efficiency than BP with sufficient parallelization. Furthermore, PCNs can be mathematically considered a superset of traditional feedforward neural networks (FNNs), significantly extending the range of trainable architectures. As inherently probabilistic (graphical) latent variable models, PCNs provide a versatile framework for both supervised learning and unsupervised (generative) modeling that goes beyond traditional artificial neural networks. This work provides a comprehensive review and detailed formal specification of PCNs, particularly situating them within the context of modern ML methods. Additionally, we introduce a Python library (PRECO) for practical implementation. This positions PC as a promising framework for future ML innovations.

1 Introduction

Neuroscience-inspired approaches to machine learning (ML) have a long history within artificial intelligence research [34, 51, 79]. Despite the remarkable empirical advances in ML capabilities in recent years, biological learning is still superior in many ways, such as flexibility and energy efficiency [51]. As such, recent years have seen a growing call for renewed emphasis on neuroscience-inspired approaches in AI research, known as *NeuroAI* [1, 108]. This is exemplified by the rising popularity of the predictive coding (PC, also known as predictive processing) framework in computational neuroscience [22, 28, 75] and its recent entrance into the field of machine learning [60, 104]. PC represents a Bayesian perspective on how the brain processes information, emphasizing the role of probabilistic models and minimization of prediction errors in perception and learning [22, 27, 28, 75]. At its core, it suggests that the brain continually generates predictions about sensory input and updates these predictions based on incoming sensory data. By removing the predictable components, this reduces redundancy in the information processing pipeline [36].

Central to PC is the concept of *hierarchical prediction*: the lowest level of the hierarchy represents sensory data, and each higher level attempts to predict neural activity in the layer below [75]. Prediction errors, arising from discrepancies between actual and predicted activity, are propagated upward through the hierarchy, while the predictions from higher levels are propagated downwards via feedback connections; see fig. 1. In the influential work by Rao & Ballard (1999), the authors showed that such a predictive coding network (PCN) can learn statistical regularities in the input and explain several neural responses in the visual cortex [13, 22, 63, 91, 102]. Since then, the PC framework has found wide adoption across neuroscience, psychology, and philosophy [17, 90]. It is often seen as part of ‘active inference’, a broader umbrella term which aims to provide an integrated perspective on brain, cognition, and behavior [71].

Although PC was partly inspired by ML methods [18, 75], within the ML community it appears to have gone mostly unnoticed until recently. In 2017, Whittington & Bogacz applied PCNs to supervised learning tasks, revealing notable properties that connect them to traditional feedforward neural networks (FNNs). First, PCNs become *equivalent* to FNNs

Authors' Contact Information: Björn van Zwol, bjornvanzwol@gmail.com; Ro Jefferson, r.jefferson@uu.nl; Egon L. van den Broek, vandenbroek@acm.org, Utrecht University, Utrecht, The Netherlands.

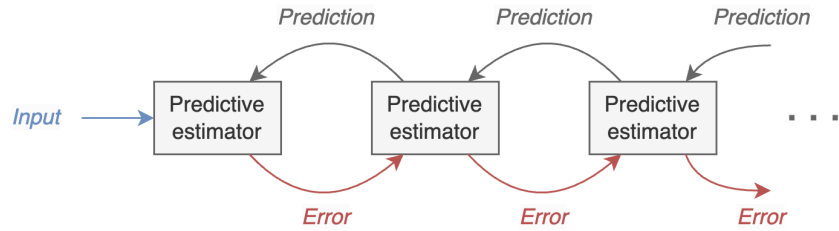


Fig. 1. **Basic PC framework**, in which the error (i.e., the discrepancy) between the actual input from lower layers and the predicted value is the information propagated upwards through the network. Figure adapted from [75].

during inference (testing) [23, 92, 104]. Second, PCN’s training algorithm, called inference learning (IL) can be related to backpropagation (BP), the workhorse training algorithm of modern deep learning. These properties sparked a surge of interest in PCNs, suggesting IL as a more biologically plausible alternative for training deep learning architectures [56, 58, 85, 86, 93].

Recent work [94] showed that IL differs from BP by using *prospective configuration*. According to this principle, neural activities across the network change before synaptic weights are modified, in order for neurons to better predict future inputs – making activity changes ‘prospective’. [94] showed that this principle naturally explains several patterns of neural activity and behavior in human and animal learning experiments which are unexplainable by BP – providing additional evidence for its biological plausibility. This property has been linked to IL’s sensitivity to second-order information in the loss landscape [5, 37], which leads to faster convergence and enhanced performance on certain learning tasks, like continual learning and online learning [6, 37, 65, 94].

Until recently, implementations of PCNs were more computationally intensive than equivalent BP-trained networks, helping to explain the lack of wider adoption of IL in ML applications. However, recent work has achieved marked improvements in performance, showing it can achieve higher efficiency than BP with sufficient parallelization [5, 87]. This is because IL’s computations use only locally available information, such that the serial updates inherent to BP can be avoided. If sufficiently parallelized, this means that computation time no longer scales with depth in PCNs [87]. As FNNs become increasingly large (deep), this could provide a marked advantage compared to BP, and further suggests PCNs are a promising candidate for use on neuromorphic hardware [60, 87].

While recent work has compared PCNs to FNNs, in particular focusing on supervised learning, fundamentally the PCN is a probabilistic (Bayesian) model, naturally formulated for *unsupervised* learning. In fact, even before it was used within ML, the PCN of Rao & Ballard was phrased in terms familiar to the ML community [53, 75]. Specifically, it is defined by a graphical model with latent (unobserved) variables, trained using generalized Expectation Maximization [7, 25], a general procedure for maximum likelihood in latent variable models (also used, e.g., in k -means clustering) [7, 19, 61]. Its objective (i.e., cost function) is the complete data log-likelihood or variational free energy when seen as a variational inference procedure [7, 26, 28]. Hence, from this perspective, PCNs are most appropriately compared not to FNNs, but to techniques associated with *generative modeling* (e.g., variational autoencoders, diffusion models [74]) and classic latent variable models (e.g., probabilistic PCA [7], factor analysis [31]). In other words, PC can be seen *both* as a learning algorithm contrasted with BP, and as a probabilistic latent variable model comparable to generative models.

In PCNs, the difference between supervised and unsupervised learning comes down to the direction of predictions within the network. In the supervised setting, these flow from data to the labels, while in the unsupervised setting,

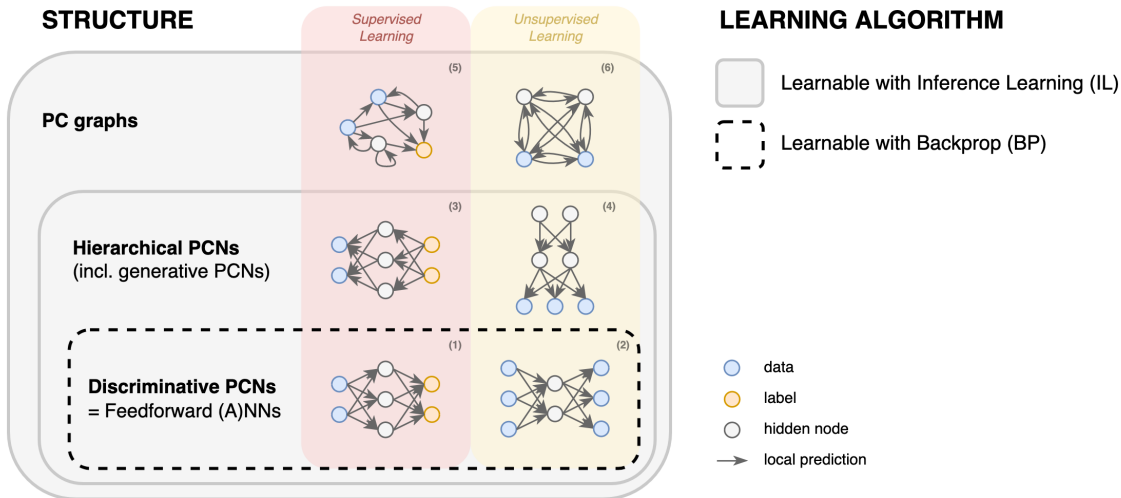


Fig. 2. **Overview of Predictive Coding Networks (PCNs).** PCNs provide a flexible framework with innovation in structure (generative PCNs, PC graphs) and learning algorithm (inference learning), compared to traditional ANNs trained with backprop. Examples of network types are schematically illustrated. The structure of PCNs and PC graphs form supersets of (feedforward) ANNs. Schematic architectures shown are: (1) multilayer perceptron/standard FNN architecture, (2) autoencoder (feedforward), (3) supervised generative PCN, (4) unsupervised generative PCN (with skip connection), (5) arbitrary PC graph, (6) fully connected PC graph.

they flow towards the data (fig. 1). Recent work [83] showed how this direction can be extended to a broader notion of *topology* by defining IL on *any graph*, known as PC graphs. This allows the training of non-hierarchical, brain-like structures, going beyond hierarchical to heterarchical prediction. This means PCNs effectively *encompass* FNNs, allowing the definition of a more general class of neural networks. While we are unaware of a formal proof in the literature, one hence expects that these networks share with FNNs the appealing property of being universal function approximators. Simultaneously, they allow a new collection of structures untrainable with BP to be studied. Although the study of such structures is in its infancy, this means they form a superset of traditional ANNs (fig. 2). This understanding of PC graphs as *generalized ANNs* follows from [83], but has not been previously phrased in this way.

The different perspectives on PCNs for ML (fig. 3) are warranted by their mathematical structure, as outlined in [10, 27, 28, 53]. Substantial progress has been made since these works, however, both theoretically and in applying PCNs to larger datasets. Although some of this progress was surveyed in [56, 60], and more recently in [81, 97], these works favor broad coverage over mathematical detail. Additionally, the only tutorial on PCNs dates from 2017 [8], before most work on PC in ML was published. Hence, there is a need for a more comprehensive formal specification, and a tutorial aimed at ML practitioners. Our work aims to provide both in the form of a combined tutorial/survey paper, as well as to clarify some minor mathematical errors in the literature.

We focus on PC as a neuro-inspired branch of ML, meaning we choose not to discuss the large body of work on PC in neuroscience, psychology, philosophy, active inference, and robotics (see aforementioned references and [44, 71] for reviews). Specifically, we do not discuss the neurologically-relevant issue of biological plausibility, often discussed in the PC literature (see e.g. [30, 94]).

In summary, the contributions of this work are as follows:

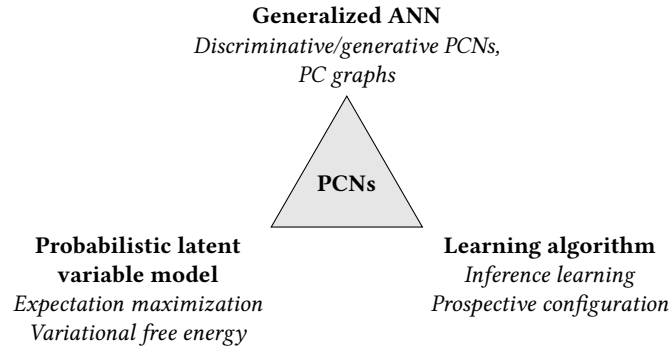


Fig. 3. **Perspectives on PCNs.**

- Provide a comprehensive formal specification of modern PCNs, clarifying some mathematical issues in earlier work.
- Summarize and provide structure for recent theoretical and empirical results on PCNs, integrating different perspectives (fig. 3), as both a unified basis for future work, and starting-point for machine learning practitioners. Our aim is to provide a technical reference while remaining accessible.
- Explain connections with existing methods in ML, some of which have remained unexposed in recent literature. In particular, we highlight how the structure of PCNs and PC graphs forms a mathematical superset of ANNs. This follows from earlier work [83], but to our knowledge was not yet pointed out as a general conception of PCNs.
- Providing a Python library (**PRECO**¹) using PyTorch that implements PCNs and PC graphs, as a hands-on tutorial.

Overview

The three perspectives in fig. 3 define the structure of this work. While interconnected, making a distinction facilitates an understanding of PCNs. Section 2 interprets PCNs as generalized ANNs (fig. 2), which should provide a familiar context for many ML researchers. Section 3 discusses PCNs as probabilistic latent variable models, and section 4 discusses work focusing on IL, i.e. PC as a learning algorithm. The literature on PCNs is organized in Table 1 by network type (section 2), which we survey throughout this work. We conclude in section 5, with appendices including an extended discussion of section 3 (appendix A), complementary proofs (appendix B.2), and a discussion of computational complexity (appendix C).

2 PCNs as Generalized ANNs

The theory of PC as a machine learning algorithm is often derived from variational inference in a hierarchical Gaussian latent variable model. The resulting equations bear a lot of similarity to those of artificial neural networks (ANNs), however. In particular, PCNs of a particular type, sometimes called *discriminative PCNs*, are in an important sense equivalent to feedforward neural network *during inference* (testing). Since we believe ANNs to be more familiar context for most ML researchers and practitioners than variational inference, we will here take ANNs as a starting point, with the aim of making the generalization to PCNs more transparent.

¹Available at <https://github.com/bjornvz/PRECO>.

Table 1. Overview of references surveyed in this work.

Subject		References	Section
Background	Existing reviews	[8, 53, 56, 60, 81]	1
	PhD theses	[4, 55, 80, 92]	
Discriminative PCNs	IL's relation to BP	[56, 57, 78, 85, 86, 93, 104, 112]	2, 4
	IL in its natural regime	[5, 23, 24, 37, 57, 58, 81, 87, 94]	
	Extensions	[12, 73, 83, 87]	
Generative PCNs	Supervised learning	[39, 83]	2.5, 3
	Unsupervised learning	[62, 65, 75, 84, 110, 111]	
Other variations and applications	Memory models	[47, 95, 96]	
	Temporal prediction	[38, 59]	
	Other	[9, 82, 100]	
Other uses of PC in ML	Neural generative coding (NGC)	[64–68]	
	PC-Inspired ANNs	[3, 14–16, 20, 33, 48, 69, 76, 106]	

Thus, we review briefly the theory of the simplest ANN: a feedforward neural network (FNN; also known as a multilayer perceptron) in a supervised learning context, as taught in introductory ML classes, after which we review discriminative PCNs. To understand similarities and differences between both networks, we discuss in detail their training procedure, learning algorithm, structure, and testing procedure.²

Problem Setup. We are given a dataset of N labelled samples $\{\mathbf{x}^{(n)}, \mathbf{y}^{(n)}\}_{n=1}^N$ split into a training set and a test set, where $\mathbf{x}^{(n)} \in X$ is a datapoint and $\mathbf{y}^{(n)} \in Y$ its corresponding label, defined on input and output domains X, Y , respectively [7].

2.1 FNNs

2.1.1 Training Procedure. FNNs are defined by a set of *activation nodes* organized in a hierarchy of L layers: $\mathbf{a}^\ell \in \mathbb{R}^{n_{\ell+1}}$, where $\ell = 0, \dots, L$ is the layer and n_ℓ the number of nodes in that layer (a constant value of 1 is added to account for the bias). Layers are connected by a set of weight matrices $\mathbf{w}^\ell \in \mathbb{R}^{n_\ell \times (n_{\ell+1}+1)}$ in the following way [7, 31]:

$$\mathbf{a}^\ell = f(\mathbf{w}^{\ell-1} \mathbf{a}^{\ell-1}), \quad (1)$$

where throughout, the biases \mathbf{b}^ℓ are absorbed as an additional column in the weight matrix (as is commonly done [31]). We will call this equation the *activity rule* since it states how activation nodes are computed. The function

²At this point, we note briefly that a second usage of term ‘PCN’ exists, referring to backprop-trained ANNs with an architecture that *takes inspiration from PC*, e.g. includes separate top-down and bottom-up FNNs (cf. ‘PC-inspired ANNs’ in table 1).

$f : \mathbb{R}^{n_\ell} \rightarrow \mathbb{R}^{n_\ell}$ here is a nonlinear activation function (e.g. sigmoid, ReLU). Setting the bottom layer \mathbf{a}^0 to a datapoint $\mathbf{x}^{(n)}$, the final layer \mathbf{a}^L is taken as the predicted label $\hat{\mathbf{y}} = \hat{\mathbf{y}}(\mathbf{w}, \mathbf{x}^{(n)})$. Then, notice that the neural network is simply a function $\text{NN} : X \rightarrow Y$, such that $\hat{\mathbf{y}} = \text{NN}(\mathbf{x}^{(n)})$ and

$$\text{NN}(\mathbf{x}) = \left(\mathbf{a}^L \circ \mathbf{a}^{L-1} \circ \dots \circ \mathbf{a}^1 \right) (\mathbf{x}). \quad (2)$$

Thus, an FNN is a function composition of linear and nonlinear operations defined through (1). The produced output $\hat{\mathbf{y}}$ is compared to the true label $\mathbf{y}^{(n)}$ using a *loss function*:

$$\mathcal{L}(\mathbf{w}) = \frac{1}{N} \sum_{n=1}^N \mathcal{L}_n(\hat{\mathbf{y}}, \mathbf{y}^{(n)}),$$

where the dependence on weights is through $\hat{\mathbf{y}}$ (note that the sum here is over the datapoints, to simplify the comparison with PCNs; typically, with mini-batch learning, one sums over the batches instead). In practice, the loss is often chosen based on properties of the task, e.g., the Mean Squared Error (MSE) loss $\mathcal{L}_n(\mathbf{y}^{(n)}, \hat{\mathbf{y}}) = \left(\hat{\mathbf{y}} - \mathbf{y}^{(n)} \right)^2$ is useful for regression-type learning.³ Then, the optimal weights are those that minimize the loss function, which defines the *learning rule* for ANNs. Since \mathcal{L} is generically a complicated non-convex function of the weights, determining an optimal set of weights can only be done numerically with gradient descent:

$$\hat{\mathbf{w}}^\ell = \underset{\mathbf{w}}{\text{argmin}} \mathcal{L}(\mathbf{w}) \implies \Delta \mathbf{w}^\ell = -\alpha \frac{\partial \mathcal{L}}{\partial \mathbf{w}^\ell}, \quad (3)$$

where the weights are updated iteratively using $\Delta \mathbf{w}^\ell$, with α the learning rate, and we use a hat to denote the optimized values. For better training efficiency, in practice one uses optimizers such as stochastic gradient descent (SGD) or Adam [40].

2.1.2 Learning Algorithm. Calculating these weights efficiently is done using backpropagation or backprop (BP), which is the standard workhorse algorithm used in deep learning. In BP, the *error* in layer ℓ is the derivative of the loss w.r.t. the activation \mathbf{a}^ℓ , i.e.

$$\delta^\ell = \frac{\partial \mathcal{L}}{\partial \mathbf{a}^\ell}. \quad (4)$$

It can be shown (appendix B.1) that the right-hand side of (3) is

$$\Delta \mathbf{w}^\ell = \alpha \delta^{\ell+1} \odot f'(\mathbf{w}^\ell \mathbf{a}^\ell) (\mathbf{a}^\ell)^T, \quad (5)$$

where

$$\delta^\ell = \begin{cases} \mathbf{a}^L - \mathbf{y}^{(n)} & \ell = L \\ (\mathbf{w}^\ell)^T \delta^{\ell+1} \odot f'(\mathbf{w}^\ell \mathbf{a}^\ell) & \ell < L \end{cases}. \quad (6)$$

Observe how errors are computed from the final to the first layer, explaining the name backpropagation of errors. Pseudocode is shown in alg. 1.

2.1.3 Structure. Fig. 4 shows the typical way to visualize an FNN. Connections are defined by (1). As such, we can say that this equation defines the *structure* of the network.

³The loss can also be derived by maximizing the likelihood function of the model, given assumptions on output variables: assuming the outputs are Gaussian random variables (appropriate for regression) leads to the MSE loss, and assuming they are Bernoulli random variables (appropriate for classification) leads to the cross-entropy loss.

Algorithm 1 Learning $\{\mathbf{x}^{(n)}, \mathbf{y}^{(n)}\}$ with BP

Require: $\mathbf{a}^0 = \mathbf{x}^{(n)}$.
 1: **for** $\ell = 0$ to $L - 1$ **do** // Forward pass
 2: $\mathbf{a}^{\ell+1} = f(\mathbf{w}^\ell \mathbf{a}^\ell)$
 3: **end for**
 4: $\delta^L = \frac{\partial \mathcal{L}}{\partial \mathbf{a}^L}$
 5: **for** $\ell = L - 1$ to 0 **do** // Backward pass
 6: $\delta^\ell = (\mathbf{w}^{\ell+1})^T \delta^{\ell+1} \odot f'(\mathbf{w}^\ell \mathbf{a}^\ell)$
 7: $\mathbf{w}^\ell \leftarrow \mathbf{w}^\ell - \alpha \frac{\partial E}{\partial \mathbf{w}^\ell}$ // Weight update
 8: **end for**

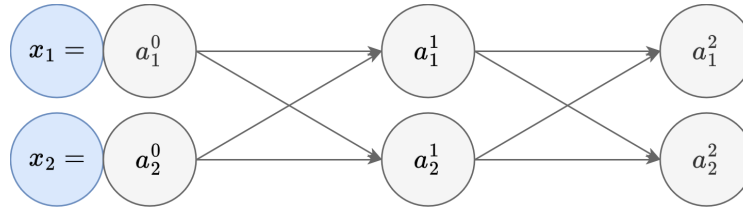


Fig. 4. **Schematic FNN structure.** A single hidden layer is shown. The connections are defined by (1), the input layer \mathbf{a}^0 is clamped to a datapoint $\mathbf{x}^{(n)}$, and the final layer \mathbf{a}^2 here is the predicted output, $\hat{\mathbf{y}}$.

2.1.4 *Testing Procedure.* Finally, after a network has been trained, *testing*⁴ the network is done by using the activity rule (1) to obtain predicted outputs $\hat{\mathbf{y}}$ from datapoints $\mathbf{x}^{(n)}$.

2.2 Discriminative PCNs

Before explaining PCNs in detail we briefly mention a convention issue. The literature contains conflicting notions of *direction* in PCNs, which are worth discussing at the outset.

Direction in PCNs. There are two connected issues, the first being mathematical: should local predictions μ^ℓ be defined as $\mu^\ell = f(\mathbf{w}^{\ell+1} \mathbf{a}^{\ell+1})$ (implied by fig. 1) or $\mu^\ell = f(\mathbf{w}^{\ell-1} \mathbf{a}^{\ell-1})$ (as in this section)? The second issue is terminological: how should the words *forward/backward* be used?

Typically in the neuroscientific PC literature [27, 75], predictions are $\mu^\ell = f(\mathbf{w}^{\ell+1} \mathbf{a}^{\ell+1})$, and data is clamped to $\ell = 0$ (fig. 1). This means that predictions go *towards data* (and errors go away from data). In this ‘PC convention’, the word *forward* is typically chosen to mean away from the data, which is the direction of errors [75]. However, in the supervised learning context, for a PCN to be equivalent to FNNs during testing, it turns out that one needs to have *predictions* go away from data. With the conventions above, this means one would have to clamp data to the highest layer $\ell = L$, which is confusing from the perspective of standard ML. This also leads to ambiguity as to whether ‘forward’ should mean towards increasing layer number, or away from the data.

The alternative when comparing PCNs to FNNs is to keep data clamped to $\ell = 0$ but *change the direction of local prediction* to $\mu^\ell = f(\mathbf{w}^{\ell-1} \mathbf{a}^{\ell-1})$, as is done by many recent works [5, 6, 12, 37, 56–58, 73, 78, 86, 94, 110]. *Forward*

⁴Note that ‘testing’ is often more generally called ‘inference’, to refer to use of a network *after* it has been trained. To prevent confusion with the inference phase *during* learning in PCNs, we refrain from using this term here.

then means away from the data (equivalently, towards higher layers) as in the PC convention above, except that this is now the direction of predictions. In other words, rather than swapping the data clamping from $\ell = 0$ to L , we instead swap the directions of predictions and errors relative to fig. 1, so that – when comparing PCNs to FNNs specifically – predictions go forwards and errors go backwards.

The disadvantage of this choice is that $\boldsymbol{\mu}^\ell = f(\mathbf{w}^{\ell+1}\mathbf{a}^{\ell+1})$ with data at $\ell = 0$ remains the more sensible convention for PCNs when seen as Bayesian/generative models (section 3) [62, 65, 75, 84]; it is only in the comparison with FNNs where some inversion (either of clamping or of directions) is required. Hence, in this work we use both conventions *depending on the use of the network*. We define *discriminative PCNs* as $\boldsymbol{\mu}^\ell = f(\mathbf{w}^{\ell-1}\mathbf{a}^{\ell-1})$ (for supervised learning), and *generative PCNs* as $\boldsymbol{\mu}^\ell = f(\mathbf{w}^{\ell+1}\mathbf{a}^{\ell+1})$ (for unsupervised learning). As for terminology, we can then unambiguously use ‘forward’ to mean *away from the data* in all cases, consistent with standard ML. One must simply bear in mind that for discriminative PCNs, ‘forward’ reflects the direction of predictions, while for generative PCNs it refers to the direction of errors.

2.2.1 Training Procedure. As with FNNs, we define activity nodes \mathbf{a}^ℓ . In line with the fundamental notion of PC, the layer $\mathbf{a}^{\ell-1}$ now tries to ‘predict’ this activity. The *local prediction* is defined as

$$\boldsymbol{\mu}^\ell = f(\mathbf{w}^{\ell-1}\mathbf{a}^{\ell-1}) \quad (7)$$

(not to be confused with the ‘global’ prediction $\hat{\mathbf{y}}$ of the network as a whole).⁵ The weights and biases are defined just like in FNNs. The discrepancy between actual and predicted activity is

$$\boldsymbol{\epsilon}^\ell = \mathbf{a}^\ell - \boldsymbol{\mu}^\ell \quad (8)$$

i.e. the *prediction error*. The objective function in PC is the sum of squared prediction errors:

$$E(\mathbf{a}, \mathbf{w}) = \frac{1}{2} \sum_{\ell} (\boldsymbol{\epsilon}^\ell)^2, \quad (9)$$

often called the *energy function*.⁶ Training now happens by setting the bottom layer \mathbf{a}^0 to the datapoint $\mathbf{x}^{(n)}$, like in FNNs, and additionally fixing the final layer \mathbf{a}^L to the correct label $\mathbf{y}^{(n)}$. The activity rule is not defined as in (1); instead, the updated values of the hidden (unclamped) activity nodes (i.e. $\ell = 1, \dots, L-1$) are the minimum of the energy function:

$$\hat{\mathbf{a}}^\ell = \underset{\mathbf{a}^\ell}{\operatorname{argmin}} E(\mathbf{a}, \mathbf{w}). \quad (10)$$

This is called the *inference phase*, since we are *inferring* the appropriate activation values for hidden nodes, given the clamped nodes (cf. section 3 for a details of the probabilistic interpretation).

⁵Writing out bias, we here use $\boldsymbol{\mu}^\ell = f(\mathbf{w}^{\ell-1}\mathbf{a}^{\ell-1} + \mathbf{b}^{\ell-1})$, which is the most common convention in ML [31, 74]. Most works in the PC literature however, define predictions as $\boldsymbol{\mu}^\ell = \mathbf{w}^{\ell-1}f(\mathbf{a}^{\ell-1}) + \mathbf{b}^{\ell-1}$, whereas the main publicly available implementation uses yet another definition: $\boldsymbol{\mu}^\ell = f(\mathbf{w}^{\ell-1}\mathbf{a}^{\ell-1}) + \mathbf{b}^{\ell-1}$ [99]. This choice of convention often does not make a difference for performance, but it is worth noting that it does change the form of the update rules. Also, the choice for the last layer is of great practical importance, since it determines the domain of possible outputs (e.g. a sigmoid or softmax is appropriate for classification but fatal for regression).

⁶In the probabilistic latent variable model perspective (section 3) this is the *complete data log-likelihood*. Section 3.4.3 further discusses the use of the term ‘energy’.

Typically, finding the minimum $\hat{\mathbf{a}}^\ell$ requires gradient descent (an important exception is the testing of discriminative PCNs, as will be discussed below). Taking the derivative using (9), one obtains:

$$\begin{aligned}\Delta \mathbf{a}^\ell &= -\gamma \frac{\partial E}{\partial \mathbf{a}^\ell} \\ &= -\gamma \left(\boldsymbol{\epsilon}^\ell - (\mathbf{w}^\ell)^T \boldsymbol{\epsilon}^{\ell+1} \odot f'(\mathbf{w}^\ell \mathbf{a}^\ell) \right)\end{aligned}\quad (11)$$

Here, γ is the *inference rate*: a step size required by gradient descent (i.e., the learning rate for activation nodes). As such, to find $\hat{\mathbf{a}}^\ell$ during training, one does T iterations of (11) until convergence.

The weights are now found at the minimum of the *same* energy function, which defines a learning rule similar to FNNs:

$$\hat{\mathbf{w}}^\ell = \underset{\mathbf{w}^\ell}{\operatorname{argmin}} E(\hat{\mathbf{a}}, \mathbf{w}) \implies \Delta \mathbf{w}^\ell = -\alpha \frac{\partial E}{\partial \mathbf{w}^\ell}, \quad (12)$$

again using a hat for the values after minimizing, and a step-wise gradient descent updates which can be done using SGD or Adam. The fact that (11) is trained to convergence before the weight update is performed suggests that training a PCN is more computationally costly than FNNs. However, this added cost can be at least partially circumvented in practice, as we discuss below. Additionally, note that since the energy function is a sum over layers, the update rule does not require backpropagating errors. Instead, taking the derivative in (9) simply gives:

$$\Delta \mathbf{w}^\ell = \alpha \boldsymbol{\epsilon}^{\ell+1} \odot f'(\mathbf{w}^\ell \hat{\mathbf{a}}^\ell) (\hat{\mathbf{a}}^\ell)^T, \quad (13)$$

i.e., the weight updates can be computed using the error and activation nodes in neighboring layers. This means PCNs' computations are local both in space and time. We discuss the advantages of this property below.

2.2.2 Learning Algorithm. By virtue of the use of the energy function for both activation updates and weight updates, training PCNs is not done by backprop, but a different learning algorithm. Pseudocode is shown in alg. 2. This is sometimes called *inference learning* (IL) [5, 6, 84] or, rarely, *prospective configuration* [94], but is often simply referred to as 'predictive coding' [83, 87]. Importantly, it is an instance of *expectation maximization* (EM) (see section 3). We choose the term IL in this work. Note that unlike BP, IL requires *initializing hidden nodes* before inference. This is often done using a 'feedforward pass', setting $\mathbf{a}^\ell(0) = \boldsymbol{\mu}^\ell$. This causes the error throughout the network to be zero except at the final layer. Other initializations can also be used [23].

Algorithm 2 Learning $\{\mathbf{x}^{(n)}, \mathbf{y}^{(n)}\}$ with IL.

Require: $\mathbf{a}^0 = \mathbf{x}^{(n)}, \mathbf{a}^L = \mathbf{y}^{(n)}$	// Clamp data
Require: $\mathbf{a}^\ell(0) = \boldsymbol{\mu}^\ell$ for $\ell = 1, \dots, L-1$	// Feedforward initialization
1: for $t = 0$ to T do	// Inference
2: for each ℓ do	
3: $\mathbf{a}^\ell(t+1) = \mathbf{a}^\ell(t) - \gamma \frac{\partial E}{\partial \mathbf{a}^\ell}$	// Activation update
4: end for	
5: end for	
6: for each ℓ do	
7: $\mathbf{w}^\ell \leftarrow \mathbf{w}^\ell - \alpha \frac{\partial E}{\partial \mathbf{w}^\ell}$	// Weight update
8: end for	

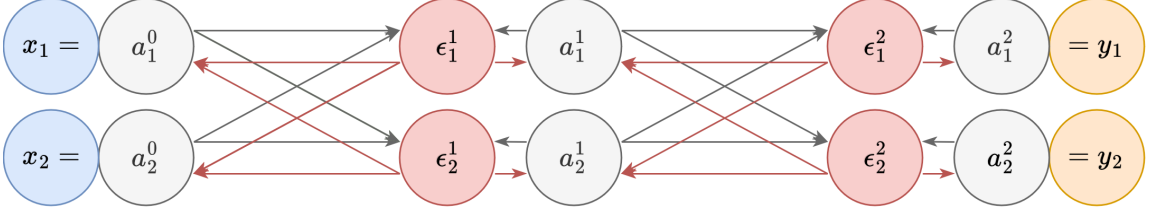


Fig. 5. **Schematic discriminative PCN structure.** A single hidden layer is shown. Grey connections correspond to updates of error nodes, defined by (7) and (8). Red connections correspond to updates of activation nodes, defined by (11). The input layer \mathbf{a}^0 is clamped to a datapoint $\mathbf{x}^{(n)}$, and the final layer \mathbf{a}^2 to the label $\mathbf{y}^{(n)}$.

Importantly, recent work introduced *incremental PC* [87] using the insight that EM admits the use of partial steps, meaning that the minimization of E w.r.t. activations does not have to be complete for the algorithm to converge. Thus, a minor change in alg. 2 gives alg. 3, which we refer to as *incremental IL* in this work.

Algorithm 3 Learning $\{\mathbf{x}^{(n)}, \mathbf{y}^{(n)}\}$ with Incremental IL.

Require: $\mathbf{a}^0 = \mathbf{x}^{(n)}, \mathbf{a}^L = \mathbf{y}^{(n)}$ // Clamp data
Require: $\mathbf{a}^\ell(0) = \boldsymbol{\mu}^\ell$ for $\ell = 1, \dots, L-1$ // Feedforward initialization

- 1: **for** $t = 0$ to T **do**
- 2: **for** each ℓ **do**
- 3: $\mathbf{a}^\ell(t+1) = \mathbf{a}^\ell(t) - \gamma \frac{\partial E}{\partial \mathbf{a}^\ell}$ // Activation update
- 4: $\mathbf{w}^\ell \leftarrow \mathbf{w}^\ell - \alpha \frac{\partial E}{\partial \mathbf{w}^\ell}$ // Weight update
- 5: **end for**
- 6: **end for**

2.2.3 *Structure.* A PCN is typically visualized as in fig. 5. The grey connections are the predictions defined by (7) (similar to those in FNNs, see fig. 4), together with error computations, (8). The red connections are defined by (11).

2.2.4 *Testing Procedure.* A PCN can be tested by clamping the lowest layer \mathbf{a}^0 to the data, and computing updates for all the other layers, now including the final layer \mathbf{a}^L , using the activity rule (10). Interestingly, computing these updates is much simpler than during training. With the output nodes now unclamped, (10) has an analytical solution. One can show [92, 104] (see appendix B.2) that with $\mathbf{a}^0 = \mathbf{x}^{(n)}$, the minimum of E is:

$$\hat{\mathbf{a}}^1 = f(\mathbf{w}^0 \mathbf{x}^{(n)}), \quad \hat{\mathbf{a}}^2 = f(\mathbf{w}^1 \hat{\mathbf{a}}^1), \quad \dots \quad \hat{\mathbf{a}}^L = f(\mathbf{w}^{L-1} \hat{\mathbf{a}}^{L-1}). \quad (14)$$

In other words, during testing, a prediction of the network can be computed using a single pass through the network, without requiring gradient-based optimization of activation nodes of (11). In other words, we can even say that testing is equivalent in PCNs and FNNs, or that during testing the PCN ‘becomes’ an FNN in the sense of (2). As such, important results for neural networks such as universal approximation theorems [74] also hold for discriminative PCNs. For these networks, the difference w.r.t. FNNs is only in their *learning algorithm*. We emphasize that this holds only for *discriminative* PCNs, with the local prediction defined as in (7), and data clamped to \mathbf{a}^0 . If this is changed, as will be done in later sections, then this equivalence no longer holds.

Table 2. **Training & testing procedures compared:** FNNs vs. discriminative PCNs. Key steps and corresponding equations are shown, and biases are omitted for clarity. ‘Fixed output’ refers to the final activity layer \mathbf{a}^L , clamped to data $\mathbf{y}^{(n)}$ during training (absent in FNNs). ‘Predicted output’ is the prediction in the final layer, $\boldsymbol{\mu}^L$, which becomes an output during testing, $\boldsymbol{\mu}^L = \hat{\mathbf{y}}$.

	Training Procedure		Testing Procedure	
	FNN	Discriminative PCN	FNN	Discriminative PCN
Input (fixed)	$\mathbf{a}^0 = \mathbf{x}^{(n)}$	$\mathbf{a}^0 = \mathbf{x}^{(n)}$	$\mathbf{a}^0 = \mathbf{x}^{(n)}$	$\mathbf{a}^0 = \mathbf{x}^{(n)}$
Output (fixed)	–	$\mathbf{a}^L = \mathbf{y}^{(n)}$	–	–
Activity rule	$\mathbf{a}^\ell = f(\mathbf{w}^{\ell-1} \mathbf{a}^{\ell-1})$	$\hat{\mathbf{a}}^\ell = \underset{\mathbf{a}^\ell}{\operatorname{argmin}} E(\mathbf{a}, \mathbf{w})$	$\mathbf{a}^\ell = f(\mathbf{w}^{\ell-1} \hat{\mathbf{a}}^{\ell-1})$	$\hat{\mathbf{a}}^\ell = \underset{\mathbf{a}^\ell}{\operatorname{argmin}} E(\mathbf{a}, \mathbf{w})$ $= f(\mathbf{w}^{\ell-1} \hat{\mathbf{a}}^{\ell-1})$
Output (predicted)	$\hat{\mathbf{y}} = \mathbf{a}^L$	$\hat{\mathbf{y}} = \boldsymbol{\mu}^L$	$\hat{\mathbf{y}} = \mathbf{a}^L = f(\mathbf{w}^{L-1} \mathbf{a}^{L-1})$	$\hat{\mathbf{y}} = \boldsymbol{\mu}^L = f(\mathbf{w}^{L-1} \hat{\mathbf{a}}^{L-1})$
Objective	$(\hat{\mathbf{y}} - \mathbf{y}^{(n)})^2$	$(\hat{\mathbf{y}} - \mathbf{y}^{(n)})^2 + \sum_{\ell=1}^{L-1} (\epsilon^\ell)^2$	$(\hat{\mathbf{y}} - \mathbf{y}^{(n)})^2$	$(\hat{\mathbf{y}} - \mathbf{y}^{(n)})^2$
Learning rule	$\hat{\mathbf{w}}^\ell = \underset{\mathbf{w}^\ell}{\operatorname{argmin}} \mathcal{L}(\mathbf{w})$	$\hat{\mathbf{w}}^\ell = \underset{\mathbf{w}^\ell}{\operatorname{argmin}} E(\hat{\mathbf{a}}, \mathbf{w})$	–	–

2.3 FNNs vs Discriminative PCNs

Here, we summarize the similarities and differences between FNNs and PCNs, reiterating the training & testing procedures, the learning algorithm, and structure.

2.3.1 Training & Testing Procedures. Table 2 summarizes the important steps and computations for FNNs (with MSE loss) and discriminative PCNs. Notice the *equality* between the MSE loss and PCN’s energy function during testing, and their *similarity* during training. This is a result of fixing the final layer of the PCN \mathbf{a}^L to the label $\mathbf{y}^{(n)}$, and labelling the prediction of the last layer $\boldsymbol{\mu}^L = f(\mathbf{w}^{L-1} \mathbf{a}^{L-1})$ as $\hat{\mathbf{y}}$. The term $\sum_{\ell=1}^{L-1} (\epsilon^\ell)^2$ is called the *internal error* [57] or *residual error* [58].

2.3.2 Learning Algorithms. Table 3 shows the key steps involved in BP and IL. The main difference is the forward ($1 \rightarrow L$) and backward ($L \rightarrow 1$) sweeps of BP, absent in IL. In contrast, updates in IL (for both activations and weights) use only local information. Updates are local in time: all layers could in principle be updated in parallel (see fig. 6). In contrast, in BP, weight updates in lower layers cannot be done before computations in all higher layers have been completed. BP thus involves waiting times; it is not local in time. If this parallelization of computation can be realized, this difference implies a potential speed-up of IL compared to BP. It should be noted that the learning time in practice involves several additional factors, discussed further in section 4.

A final note on learning concerns weight initialization. It is well-known in machine learning that in deep networks, correctly initializing weights is required for networks to be trainable [11, 31, 74, 89]. This has not yet been studied in relation to PC except [23], which only showed that weights ought to be sufficiently small at initialization. Practical uses

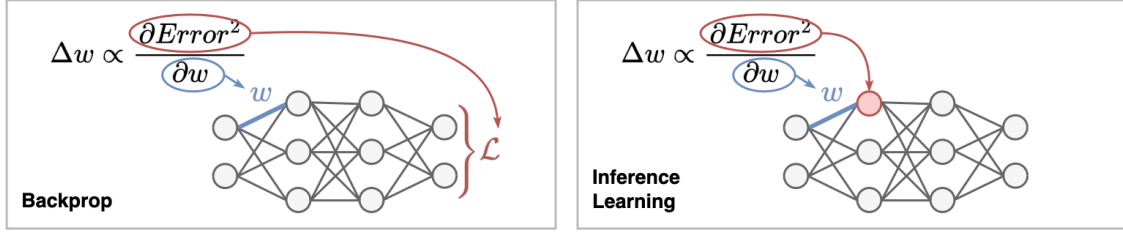


Fig. 6. **Locality in IL.** Schematic illustration of weight updates BP in an FNN vs. IL in a PCN. In the former, the cost or loss function \mathcal{L} plays the role of the (squared) error in this example, which must be propagated from the output layer all the way back through the network until the relevant weight is reached; in contrast, in IL the errors are locally computed. This is often cited as a reason for the greater biological plausibility of PCNs, but is practically relevant insofar as it allows the updates to be performed in parallel, and avoids issues surrounding vanishing/exploding gradients. Figure adapted from [56].

Table 3. **Learning algorithms compared:** backprop (BP) in an FNN vs. inference learning (IL) in a discriminative PCN. Whereas the form of equations are similar in both algorithms, they are conceptually different. BP proceeds in a backward and forward phase, such that nodes in lower layers need to wait for the error computed at the output to be propagated back. IL has no such waiting times since layers can be updated in parallel. At the same time, processing a batch in BP is done by a single forward and backward pass, while in IL this requires several inference.

Backprop		Inference Learning	
Forward pass	$\mathbf{a}^\ell = f(\mathbf{w}^{\ell-1} \mathbf{a}^{\ell-1}) \quad \ell : 1 \rightarrow L$	Inference	$\boldsymbol{\mu}^\ell = f(\mathbf{w}^{\ell-1} \mathbf{a}^{\ell-1})$
Backward pass	$\left. \begin{aligned} \boldsymbol{\delta}^\ell &= \frac{\partial \mathcal{L}}{\partial \mathbf{z}^\ell} \\ &= (\mathbf{w}^\ell)^T \boldsymbol{\delta}^{\ell+1} \odot f'(\mathbf{w}^\ell \mathbf{a}^\ell) \end{aligned} \right\} \ell : L \rightarrow 1$		$\boldsymbol{\epsilon}^\ell = \mathbf{a}^\ell - \boldsymbol{\mu}^\ell$
Learning	$\Delta \mathbf{w}^\ell = \alpha \boldsymbol{\delta}^{\ell+1} \odot f'(\mathbf{w}^\ell \mathbf{a}^\ell) (\mathbf{a}^\ell)^T$		$\Delta \mathbf{a}^\ell = -\gamma \left(\boldsymbol{\epsilon}^\ell - (\mathbf{w}^\ell)^T \boldsymbol{\epsilon}^{\ell+1} \odot f'(\mathbf{w}^\ell \mathbf{a}^\ell) \right)$
		Learning	$\Delta \mathbf{w}^\ell = \alpha \boldsymbol{\epsilon}^{\ell+1} \odot f'(\mathbf{w}^\ell \hat{\mathbf{a}}^\ell) (\hat{\mathbf{a}}^\ell)^T$

so far (e.g., [94]) and publicly available implementations [99] use a value of 0.05, similar to typical values chosen for ANNs [72], but this choice lacks a theoretical basis, and more optimal initialization schemes may exist.

2.3.3 Structure. A typical representation of the structure of an FNN is a diagram like in fig. 4. The connections in this diagram are unambiguously defined by the activity rule (1). The learning algorithm (BP) is defined by (3) and (4) (typically not included in visual representations). In this way, FNNs admit some degree of independence between the notions of structure and learning algorithm. In contrast, PCNs do not (yet) have a universally employed visual representation, although most diagrams are similar to fig. 5. Observe that PCNs have bottom-up connections from data to labels (predictions), as well as top-down connections from labels to data (errors), meaning they have *feedback/recurrence*⁷ in all nodes, a fundamental feature of PC. Note however, that (for discriminative PCNs) these feedback components are only used during training (cf. section 2.2.4). For PCNs, structure and learning algorithm are more difficult to separate (cf. appendix B.3).

⁷It is also worth emphasizing that this recurrence is of an altogether different nature than that in recurrent neural networks (RNNs) [31], where the recurrence is in time rather than in spatial connectivity (i.e., RNNs are characterized by weight sharing). In PCNs, time steps are iterations in the inference phase, whereas in RNNs, time steps are subsequent samples of temporal data. A variation of PCNs applied to temporal data is [59].

Table 4. **Time Complexity for BP, IL, and incremental IL/incremental PC.** M is the most costly matrix computation, T is the number of steps to convergence, and L is the number of layers (i.e., depth). As discussed above, the local nature of IL allows parallelization to remove the dependence on depth, which is not possible in BP.

	BP	IL	Incremental IL
Standard	$O(LM)$	$O(TLM)$	$O(LM)$
Parallelized	$O(LM)$	$O(TM)$	$O(M)$

2.3.4 *Computational Complexity.* Since testing a FNN and PCN is equivalent, their time complexity during this phase is equal. As for the training phase, by studying the computations in table 3, the time complexity of a single weight update can be computed (reviewed in detail in appendix C). The results of these computations are summarized in table 4. With matrix multiplications being the most costly computations and defining M as the complexity for the largest weight multiplication, the complexity can be shown to be $O(LM)$ for BP, $O(TLM)$ for IL and $O(LM)$ for Incremental IL [5, 87]. That is, BP and incremental IL have the same time complexity per weight update, with standard IL a factor of T more costly.

However, as mentioned above, the computations in IL enjoy both temporal and spatial locality, meaning the computations in different layers during inference and learning could be parallelized. Ignoring overhead, this implies that IL’s time complexity would decrease to $O(TM)$, and incremental IL would have $O(M)$, which is faster than BP. In this case, total training time no longer scales with the depth of the network, which is a highly desirable feature. A first implementation of this kind was provided by [87]. However, their algorithm included a substantial computational overhead, such that it is only faster in networks where $L \gtrsim 128$. At the same time, BP is heavily optimized by dedicated libraries that employ GPU acceleration, whereas no similarly comprehensive library yet exists for IL. In addition, note that the time complexity per weight update is not the only factor that determines training time in practice: the second key factor is the number of epochs until convergence, which depends on the optimizer, dataset, and other hyperparameters used. These can impact the learning properties of BP and IL in different ways. We discuss some of these topics in section 4.

2.3.5 *Empirical Results.* As is well known to deep learning practitioners, many factors affect performance of FNNs, which is no different with discriminative PCNs. Exponential growth of the search space with hyperparameters makes a systematic comparison intractable, meaning existing works compare FNNs and PCNs only over a small range of hyperparameters. Interestingly, discriminative PCNs often perform extremely similar to FNNs [94, 104], but works by [23, 24] also make clear that care needs to be taken in importing knowledge and intuitions from BP-trained networks since IL does introduce meaningful changes related to its mathematical properties. With this remark we summarize the advantages and limitations that have been observed so far.

In terms of improvements of PCNs over FNNs, most noteworthy are those observed in [94] and [6]. Ref. [94] observes minor but statistically significant improvements for *online learning* (learning with batch size 1) and *data efficiency* (learning with less than 300 data points per class), on the order of 2% in the best case. Gains in classification accuracy of this order is also observed in [6], who additionally observe that the use of optimizer greatly affects results, exhibiting differences between BP and IL. Specifically, IL combined with SGD sometimes converges to poor local minima, while BP does not (with Adam, IL again improves to the level of BP). Somewhat more impressive are the improvements observed for *continual learning* tasks and *concept drift* tasks observed in [94], with gains of 5-20%. Overall, both works generally observe faster convergence measured as number of epochs. The recent work [37] finds evidence confirming this (cf.

section 4, for further theoretical discussion). On larger architectures (e.g., for CNNs), [6] observe that IL with SGD sometimes converges to shallow local minima, such that BP outperforms IL by a large margin (order of 10%). However, this difference is decreased to 2% by using Adam.

Although IL often appears to converge in fewer epochs, its total computation time (as measured by wall-clock time) is often cited to be larger than BP, although few works have studied this extensively. Reasons for this include standard IL’s $O(TLM)$ complexity per weight update (improved with incremental IL), and an increased computational overhead. For standard IL, then, three main counteracting ‘forces’ appear to be at play: (1) decreased number of epochs required, (2) *increased* computation per weight update, and (3) *increased* overhead. With (2) largely removed in incremental IL, it remains to be studied how (1) and (3) balance out in practice.

In sum, the existing literature suggests that IL performs roughly as well as BP when measured by accuracy on typical classification tasks. IL sometimes performs worse, but this appears to be largely remedied by choice of other optimizers, where we stress again that relatively little effort has been directed towards optimization of PCNs. For specific tasks (continual learning, concept drift, and marginally so with little data and online learning), IL appears to outperform traditional ANNs trained with BP. On the matter of computation time, IL appears to converge in fewer epochs, but more extensive comparisons in wall-clock time remain to be done.

2.4 Extensions

It is straightforward to extend discriminative PCNs to more complex architectures such as convolutional neural networks [6, 85], recurrent neural networks [85], variational autoencoders and transformers [73]. Other objective functions may also be considered [58, 73].

2.4.1 Convolutional Layers. In traditional ANNs, convolutional layers replace (1) by

$$a_{ij}^{\ell+1} = f\left(\sum_{x=1}^{k_\ell} \sum_{y=1}^{k_\ell} W_{xy}^\ell a_{i+x, j+y}^\ell + b^\ell\right) \quad (15)$$

where W^ℓ is the kernel, a matrix of size $k_\ell \times k_\ell$ with k_ℓ the kernel size. For each (now two-dimensional) output neuron $a_{ij}^{\ell+1}$ one sums over x and y , the neurons in the local receptive field. W , then, is a weight matrix shared by all neurons, together with a single bias b^ℓ . Layer-dependent stride s_ℓ (which allows moving the local receptive field in larger steps) and padding of zeros p_ℓ can be introduced by setting $x \rightarrow s_\ell x - p_\ell$ and $y \rightarrow s_\ell y - p_\ell$. Importing this to PCNs, we see that we need only change the arguments of the activation functions: z^ℓ in the relations $a^\ell = f(z^\ell)$ (ANNs) and $\mu^\ell = f(z^\ell)$ (PCNs) respectively. Pooling layers (which reduce the dimensionality of layers by downsampling) can similarly be written by changing only z^ℓ .

2.4.2 Other Objective Functions, Transformers and VAEs. So far, the objective function considered was $E = \sum_\ell (\epsilon^\ell)^2$, which corresponded to the MSE loss in FNNs, $\mathcal{L}_n = (\hat{\mathbf{y}} - \mathbf{y}^{(n)})^2$. Generalizing this to any layer-dependent energy one may write $E = \sum_\ell E_\ell$, where E_ℓ may now be generalized to other functions. For instance, instead of an MSE-like error, [73] derives cross-entropy-like error:

$$E_\ell = \sum_{k=1}^K a_k^\ell \log \frac{a_k^\ell}{\mu_k^\ell}$$

which is appropriate for binary output variables. Even more generally, one may write: $E_\ell = g(a^\ell, a^{\ell-1})$ where g is some function [58].

In [73], this is used to train transformers and VAEs. Training transformers requires *attention layers* which include the softmax function. These require summing over all nodes in a layer, and are hence not included in PC as presented above, which considered only layer-dependent activations. Considering PC for non-Gaussian distributions (cf. section 3) however [73] makes this extension possible. Using a similar framework, the same authors also train variational autoencoders (VAEs) [41] with IL.

2.5 Generative PCNs

In the supervised learning context, discriminative models approximate the posterior probability distribution of labels given datapoints, $p(y|x)$ [7]. If equipped with a softmax function at the final layer, this is precisely what the model above does (hence the term discriminative PCN). Making only a minor change to the approach discussed above, one instead obtains a model that approximates $p(x|y)$: a *generative model*, from which synthetic points in the input space can be generated. Generative modeling is often done using unsupervised learning, concerned with finding patterns and structure in unlabeled data [7]. This means a change in the problem setup: one no longer has a dataset $\{\mathbf{x}^{(n)}, \mathbf{y}^{(n)}\}_{n=1}^N$, but only $\{\mathbf{x}^{(n)}\}_{n=1}^N$.

To obtain a generative PCN, one changes the structure of the network; specifically, the direction of the local predictions: $\boldsymbol{\mu}^\ell = f(\mathbf{w}^{\ell-1}\mathbf{a}^{\ell-1})$ becomes $\boldsymbol{\mu}^\ell = f(\mathbf{w}^{\ell+1}\mathbf{a}^{\ell+1})$.⁸ With IL, such a model can be used both for supervised learning, as well as unsupervised learning, with the difference being the training and testing procedures, discussed below.

In general, it should be noted that testing a generative model is less straightforward than testing discriminative models, since they can be used for several purposes (e.g. density estimation, sampling/generation, latent representation learning) [74].

2.5.1 Supervised Learning. Compared to discriminative PCNs, the *training procedure* and *learning algorithm* (IL), are unchanged: (10) is run until converged, followed by a weight update. The changed local prediction results in slight changes to update rules: in (10) and (12), $\ell + 1$ becomes $\ell - 1$. For the *testing procedure*, clamping the final layer \mathbf{a}^L to a label, with the reversed prediction direction one has the reverse of (14): a synthetic datapoint is created at \mathbf{a}^0 in a single ‘backward’ pass⁹ (without requiring several iterations of (10)).

2.5.2 Unsupervised Learning. For traditional ANNs, an FNN may be adapted for unsupervised learning by using a special autoencoder architecture, encoding input data into a lower-dimensional representation followed by a decoder which reconstructs the original input. PCNs do not require a special architecture of this sort, but only change the *direction* of prediction to $\boldsymbol{\mu}^\ell = f(\mathbf{w}^{\ell+1}\mathbf{a}^{\ell+1})$ i.e. the use of a generative PCN. Indeed, PCNs were originally conceived in this way [75] (also see section 3). The *training procedure* for unsupervised learning requires only a minor change to the approach described above. Simply keep the final layer \mathbf{a}^L *unclamped* during training, keeping data $\mathbf{x}^{(n)}$ clamped to \mathbf{a}^0 , and run IL. The model functions like an *autoencoder*: higher layers take the role of the latent space, which during training encodes increasingly abstract features of the data clamped to the lowest layer. As such, the PCN takes the role of *both* encoder and decoder.

As for the ‘testing’ procedure, one can sample the latent space as a decoder using a noise vector and *ancestral sampling*. Seeing the PCNs as a hierarchical probabilistic model (cf. section 3), each layer has a (Gaussian) conditional probability

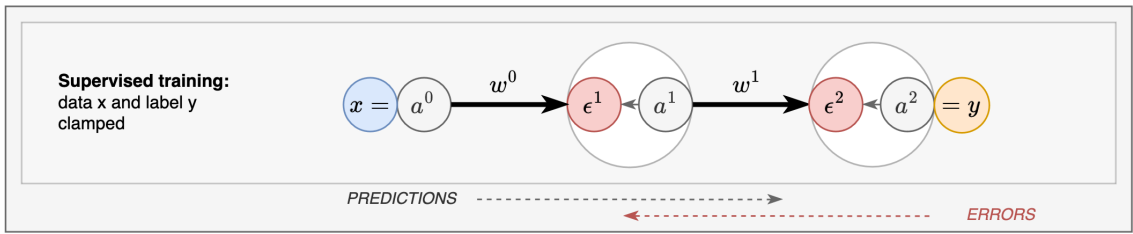
⁸Equivalently, one leaves the local predictions unchanged, and swap sides where the data and label are clamped: i.e. clamp $\mathbf{x}^{(n)}$ to \mathbf{a}^L and $\mathbf{y}^{(n)}$ to \mathbf{a}^0 , cf. section 2.2.

⁹In a generative PCN, backward is the direction of predictions (cf. section 2.2), i.e. this backward pass involves the same computations as the forward pass in an FNN.

distribution. The idea of ancestral sampling is to generate a sample from the root variable(s) (the top layer) and then sample from the subsequent conditional distributions based on this [74]. Finally, a synthetic datapoint at the bottom is obtained [65].

2.5.3 Hierarchical PCNs. Discriminative and generative PCNs can together be called *hierarchical PCNs*, defined by the local prediction $\mu^\ell = f(w^{\ell\pm 1} a^{\ell\pm 1})$. The supervised and unsupervised learning that can be done with generative PCNs can then be called the *training modes* of PCNs. These are illustrated in fig. 7. Intuitively, we can see the difference between discriminative and generative PCNs in the direction of predictions: in the discriminative model, predictions flow from data to labels, while errors flow from labels to data. In generative models, this is reversed.¹⁰

DISCRIMINATIVE PCN $\mu^\ell = f(w^{\ell-1} a^{\ell-1})$



GENERATIVE PCN $\mu^\ell = f(w^{\ell+1} a^{\ell+1})$

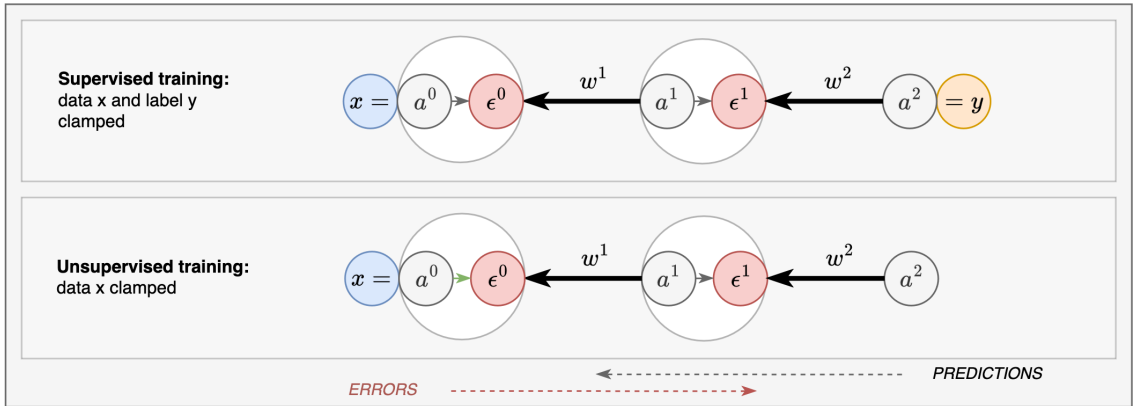


Fig. 7. **Overview of hierarchical PCNs.** Model type (discriminative vs. generative), learning mode (supervised vs. unsupervised), and direction of predictions and errors are shown. Cf. section 2.2 for an explanation of our convention. For clarity, one neuron per layer is shown, and bias has been left out.

¹⁰It should be noted that testing can also be ‘reversed’ in hierarchical PCNs, which we call *backwards testing*. If one has trained the discriminative PCN, one can clamp *labels* and find the minimum energy with iterative inference, producing a synthetic image at the bottom. Conversely, a trained generative PCN can classify images by iterative inference, using a clamped image instead of a clamped label. Thus, confusingly, discriminative PCNs can be used for generative tasks, and generative PCNs can be used for discriminative tasks. However, in practice, neither works better than their forward-tested counterpart [39, 56], meaning generative PCNs are the natural choice for generation, as discriminative PCNs are for classification. This justifies the naming convention used here and elsewhere in the literature.

2.5.4 Empirical Results. Compared to discriminative PCNs, generative PCNs remain underexplored in the literature. This is perhaps surprising considering the original conception of PC as an unsupervised generative model. At the same time, as was mentioned, metrics for what counts as a ‘good’ generative model are wide and varied [74], making it a more involved field of study in general. Indeed, the works in the literature are disparate and focus on different aspects.

Although not used for machine learning tasks, we mention [75] here as the first generative PCN trained in unsupervised mode. Then, [84] used generative PCN as an associative memory model. It was tested on the task of reconstructing from corrupted and partial data, using up to 500 datapoints. They find good performance, outperforming autoencoders, and both Hopfield networks [35] and modern Hopfield networks [43] in most cases. Another set of unsupervised tasks was considered by [65], and extended in [66]. This work used a set of models dubbed *neural generative coding* (NGC). This framework is equal in spirit to PCNs as presented in section 2, but differs in notation/terminology as well as some structural aspects. The authors study the network’s performance on reconstruction & sampling ability (as measured by the likelihood) on black and white images. They find that NGC is competitive with VAEs and GANs on these tasks, and works well on downstream classification.

Next, a smaller study [39] considers the performance of generative PCNs on standard classification tasks, training the model in supervised mode with backwards testing. Similar to [5], it is observed that the weights of different layers are updated at different rates, which causes model accuracy to worsen after it has peaked. They propose that regularizing weights remedies this pathology.

The recent work of [112] considers the sampling ability of generative PCNs trained in supervised mode with a modified training objective (cf. section A.2.3). They find that their objective improves both likelihood and sample quality, but suffers from increased computation time with results not matching performance of VAE counterparts. An improvement was presented in [111], where the inference phase is combined with Langevin sampling, giving results that match or exceed VAE performance on metrics such as FID (Fréchet Inception Distance), diversity, and coverage.

2.6 PC Graphs

The previous section showed how the structure of discriminative PCNs, could be extended by changing the definition of local prediction from $\mu^\ell = f(\mathbf{w}^{\ell-1} \mathbf{a}^{\ell-1})$ to $\mu^\ell = f(\mathbf{w}^{\ell+1} \mathbf{a}^{\ell+1})$. This can be taken one step further: PCNs can be naturally generalized to arbitrary graphs, called *PC graphs* by [83].¹¹ These are trained using IL, but dispense with the hierarchical structure of layers. These networks can be understood as a superset of both discriminative and generative PCNs, and can flexibly be used for a variety of tasks.

2.6.1 Structure. PC graphs are defined by a collection of N activation nodes $\{a_i\}_{i=1}^N$, and error nodes $\{\epsilon_i\}_{i=1}^N$, with $a_i, \epsilon_i \in \mathbb{R}$, and $\epsilon_i = a_i - \mu_i$. The local prediction is defined as:

$$\mu_i = \sum_{j \neq i} f(w_{ij} a_j),$$

where $w_{ij} \in \mathbb{R}$, and the sum is over all the other nodes, meaning self-connections are left out ($w_{ii} = 0$), as in [83]. This defines a *fully-connected* PC graph. If we choose to include self-connections one simply takes the sum over all values of i . In vector notation, one can write $\boldsymbol{\mu} = f(\mathbf{w}\mathbf{a})$.

A small PC graph is illustrated in fig. 8, where each activation node a_i and error node ϵ_i has been grouped in a *vertex* v_i . Importantly, graphs with different connectivity/topology can be obtained by multiplying the weight matrix with a

¹¹Note that PC graphs are distinct from graph neural networks (GNNs), which are used for graph-structured data [103].

mask or *adjacency matrix*. In this way, one obtains the architectures discussed in earlier sections: the discriminative PCN, as well as the generative PCN, depending on which weights are masked, cf. fig. 9.

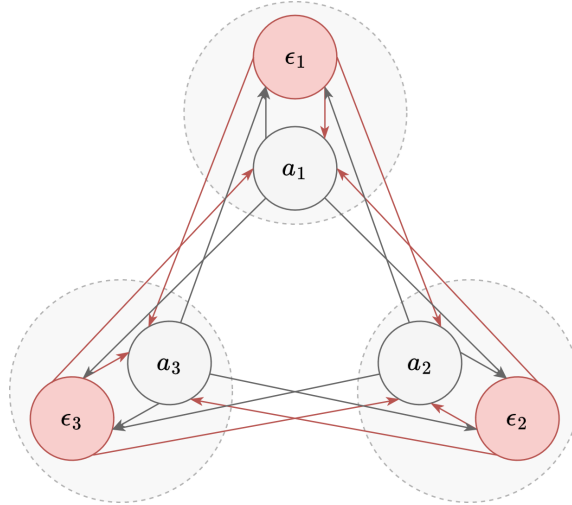


Fig. 8. **Schematic architecture of a PC graph.** Three vertices are shown in a fully connected graph without self-connections. As before, are shown as grey arrows, and error signals as red arrows. When training a PC graph, a subset of nodes is chosen for the data. If trained in supervised mode, an additional subset is chosen for the label.

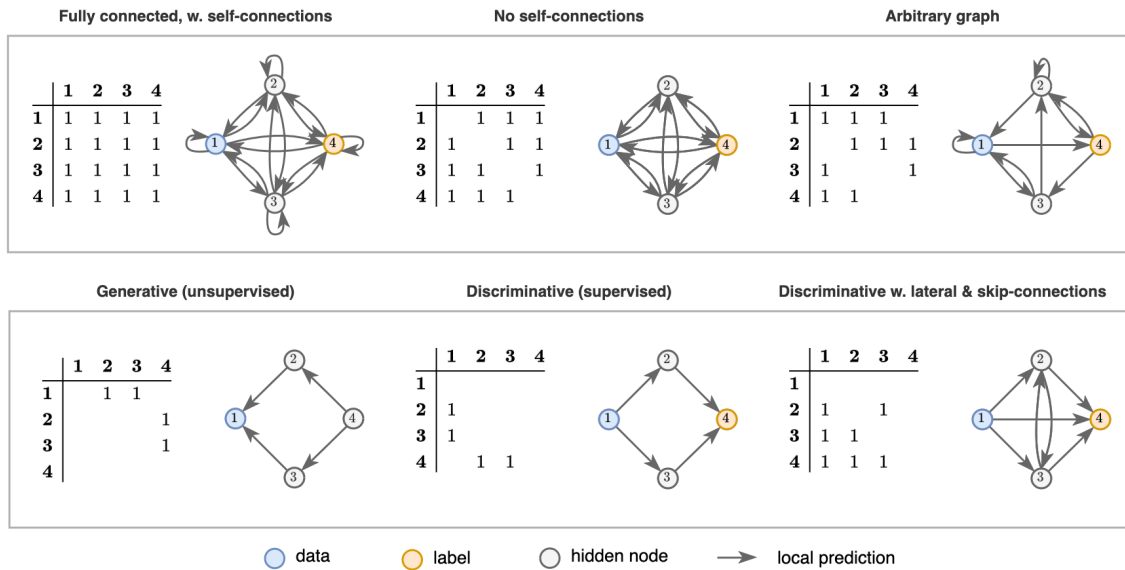


Fig. 9. **Mask/adjacency matrices for a 4-node PC graph.** Different matrices lead to different architectures, like the discriminative PCN, generative PCN, or an arbitrary topology. Larger networks are obtained in the same way. See also fig. 4 in [83].

Table 5. **Hierarchical PCNs compared to PC graphs.** The latter is a superset of the former insofar as it allows arbitrary connectivity between nodes.

	Hierarchical PCN	PC Graph
Prediction	$\boldsymbol{\mu}^\ell = f(\mathbf{w}^{\ell\pm 1} \mathbf{a}^{\ell\pm 1})$	$\boldsymbol{\mu} = f(\mathbf{w}\mathbf{a})$
Error	$\boldsymbol{\epsilon}^\ell = \mathbf{a}^\ell - \boldsymbol{\mu}^\ell$	$\boldsymbol{\epsilon} = \mathbf{a} - \boldsymbol{\mu}$
Energy	$\frac{1}{2} \sum_\ell (\boldsymbol{\epsilon}^\ell)^2$	$\frac{1}{2} \boldsymbol{\epsilon}^2$
Inference	$\Delta \mathbf{a}^\ell = -\gamma \left(\boldsymbol{\epsilon}^\ell - (\mathbf{w}^\ell)^T \boldsymbol{\epsilon}^{\ell\mp 1} \odot f'(\mathbf{w}^\ell \mathbf{a}^\ell) \right)$	$\Delta \mathbf{a} = -\gamma \left(\boldsymbol{\epsilon} - \mathbf{w}^T \boldsymbol{\epsilon} \odot f'(\mathbf{w}\mathbf{a}) \right)$
Learning	$\Delta \mathbf{w}^\ell = \alpha \boldsymbol{\epsilon}^{\ell\mp 1} \odot f'(\mathbf{w}^\ell \hat{\mathbf{a}}^\ell) (\hat{\mathbf{a}}^\ell)^T$	$\Delta \mathbf{w} = \alpha \boldsymbol{\epsilon} \odot f'(\mathbf{w}\hat{\mathbf{a}}) \hat{\mathbf{a}}^T$

2.6.2 Training Procedure. Depending on the task, different nodes in the PC graph can be clamped during training. For instance, in a standard supervised mode, the data $\{x_i\}_{i=1}^K$ (with dimensionality K) is clamped to a subset of activation nodes $\{a_i^x\}_{i=1}^K$, and the label $\{y_i\}_{i=1}^M$ (dimensionality M) is clamped to a second subset $\{a_i^y\}_{i=1}^M$. With simplified notation we can write this as:

$$\{x_i\} = \{a_i^x\} \subset \{a_i\}, \quad \{y_i\} = \{a_i^y\} \subset \{a_i\}. \quad (16)$$

For unsupervised learning, only data is clamped: $\{x_i\} = \{a_i^x\} \subset \{a_i\}$. Following this, IL can be used like earlier, where the key computations change only changing slightly. For example, the energy function becomes $E = \frac{1}{2} \sum_i (\epsilon_i)^2 = \frac{1}{2} \boldsymbol{\epsilon}^T \boldsymbol{\epsilon}$; other equations are shown in table 5. Observe that the equations are obtained by simply omitting the layer ℓ in the equations of section 2.2.

2.6.3 Testing Procedure. Depending on how the network was trained and the desired application, different nodes can be clamped also during testing. After supervised training, classification/generation of synthetic datapoints can be done by clamping a datapoint/label respectively, running inference until convergence, and considering the produced output (a label/datapoint).

2.6.4 Empirical Results. PC graphs have only been used in [83], with models trained using supervised mode only. They train models for classification, generation, reconstruction, denoising, and associative memory tasks (using different adjacency matrices). An interesting result is that for classification using a *fully connected* model, PC graphs perform much better than other fully connected architectures such as Boltzmann machines and Hopfield networks, up to 30% better on MNIST. At the same time, the fully connected model does not perform comparably to hierarchical networks trained with either BP or IL. This might be expected, considering that depth is suggested to be critical for performance in neural network learning [74]. At the same time, such statements are based mostly on empirical evidence, and lack a definitive theoretical basis. For the other tasks considered, only proofs of concepts are provided to demonstrate their flexibility. Unsupervised learning is also not considered.

2.7 Generalized ANNs

At this point it is useful to compare PC graphs with PCNs discussed in section 2. Fig. 9 illustrated how different adjacency matrices lead to the architectures discussed in earlier sections. Given the result of (14) that FNNs are equivalent to discriminative PCNs during testing, we can see them as a *subset* of hierarchical PCNs, defined by the local prediction

$\mu^\ell = f(\mathbf{w}^{\ell\pm 1} \mathbf{a}^{\ell\pm 1})$. In turn, hierarchical PCNs can be seen as a subset of PC graphs, with a particular choice of adjacency matrix.¹² This is illustrated in fig. 10, as well as fig. 2.

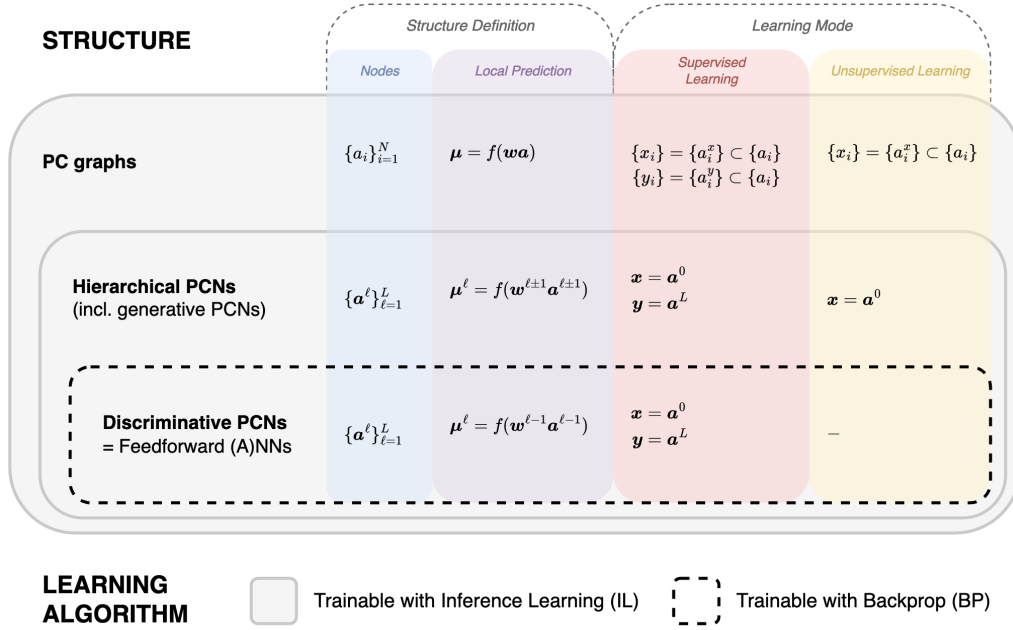


Fig. 10. **Overview of different PCNs and training modes.** Formally, the structure of PC graphs form a superset of hierarchical PCNs, which are a superset of discriminative and generative PCNs. As discussed in section 2, discriminative PCNs are equivalent to FNNs during testing; see also fig. 2.

Thus, it becomes clear that formally, PCNs and PCGs can be seen as types of ‘generalized ANNs’ that go beyond hierarchical structures, by virtue of the use of IL as opposed to BP. This is very interesting, for at least two reasons. First, as observed by [83], PC graphs allow one to train non-hierarchical structures with a brain-like topology. Speculatively, such networks could, if better understood, share some of the advantages that biological brains have over ANNs, such as vastly superior energy efficiency and parallelization. Second, from a very general perspective, topological considerations have strongly contributed to several advances in machine learning in the past. A prominent example is that of residual networks and skip connections [109], which have allowed training of much deeper networks, and can improve performance on a variety of tasks [74]. In a sense, the very notion of *depth* in deep learning is a topological feature. As such, we consider this an important avenue for further work.

3 PCNs as Probabilistic Latent Variable Models

Section 2 introduced the PCN as a type of generalized ANN. In this section we discuss a second, complementary, perspective: PCN as a *probabilistic latent variable model*. Conceptualizing PCNs in this way allows a principled derivation of equations in the previous section, and brings to light connections to other methods well-known in machine learning

¹²A small caveat to this statement is that in PC graphs, *all* value nodes have a corresponding error node, whereas in discriminative (generative) PCNs, the first (last) layer does not have its own error nodes (see fig. 7). If desired, this can be accounted for by additionally masking the corresponding errors. It should also be noted that implementing the feedforward pass initialization of hidden nodes (section 2.2.2) and feedforward inference is more complex in PC graphs.

(e.g., variational autoencoders and linear factor models). It also reveals a number of assumptions and modeling choices, providing a basis for improvements and possible future developments.

We start our step-by-step derivation from maximum likelihood estimation in probabilistic (Bayesian) models, discussing how expectation maximization (EM) implements maximum likelihood for models with latent variables, and how different generative models lead to PC as formulated by [75] or to multi-layer PC as described in the previous section.

A Brief History of PCNs. The original model of Rao & Ballard [75] was conceived as a probabilistic hierarchical model with Gaussian relations between layers. This formulation contained the ingredients typically associated with PC, chief among them the minimization of prediction errors in a hierarchical fashion. Work by Friston [25, 27, 29] showed how the computational steps in PC (minimization of the energy with respect to activations and weights) are an instance of EM, also understood as a variational inference procedure using a variational free energy (i.e., the evidence lower bound) as the objective function. This perspective explains why EM maximizes the likelihood of the data, and can be used to derive generalized objective functions (cf. appendix A).

We remark that, unlike most works in the PC literature, we emphasize the role of EM to explain IL, deferring to appendix A the derivations involving the variational free energy. We choose this focus because the two steps of IL (inference and learning) correspond precisely to the two steps of EM (expectation and maximization), and because EM is perhaps more familiar to machine learners than the thermodynamics-inspired free energy approach.

3.1 Expectation Maximization

Given data $\mathbf{x} \in \mathbb{R}^{n_x}$ (an observed variable), EM is a general method for maximizing the (log-)likelihood in models with latent variables $\mathbf{z} \in \mathbb{R}^{n_z}$, or equivalently, minimizing the negative log-likelihood,

$$\text{NLL}(\theta) = -\ln p_\theta(\mathbf{x}), \quad (17)$$

where θ are the parameters that define the model. For some joint distribution $p_\theta(\mathbf{x}, \mathbf{z})$, also called the generative model, it can be shown that the following two steps will minimize the NLL (see appendix A):

$$\tilde{\mathbf{z}} = \underset{\mathbf{z}}{\operatorname{argmax}} p_\theta(\mathbf{x}, \mathbf{z}) \quad \text{(E-step)}, \quad (18)$$

$$\hat{\theta} = \underset{\theta}{\operatorname{argmax}} p_\theta(\mathbf{x}, \tilde{\mathbf{z}}) \quad \text{(M-step)}. \quad (19)$$

Here, $\ln p_\theta(\mathbf{x}, \mathbf{z})$ is also called *complete data log-likelihood*, since it represents the likelihood function calculated using the full set of observed and latent variables – to distinguish it from the likelihood calculated only with observed data [7]. We will label the *negative complete data log-likelihood* as E :

$$E(\mathbf{x}, \mathbf{z}) = -\ln p_\theta(\mathbf{x}, \mathbf{z}) \quad (20)$$

which refers to *energy*, as in section 2 (cf. section 3.4.3 for discussion on energy-based models). We will choose to minimize E as opposed to maximizing $\ln p_\theta(\mathbf{x}, \mathbf{z})$. It has furthermore been shown (cf. appendix A, ref. [61]) that *partial*

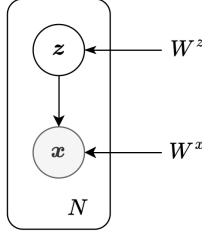


Fig. 11. **Directed graphical model for PCNs of Rao & Ballard** [75], with variances set to unity. Probabilistic graphical models represent how a joint probability distribution of random variables (nodes) can be factorized, here showing (23) with $\theta = \{W_z, W_x\}$ representing deterministic parameters. The graphical model is surrounded by a *plate* labelled with N indicating that there are N nodes of this kind, one for each datapoint (cf. e.g.[7]).

E-steps and M-steps will also minimize the NLL:

$$\Delta z \propto -\frac{\partial E}{\partial z} \quad \textbf{(partial E-step)}, \quad (21)$$

$$\Delta \theta \propto -\frac{\partial E}{\partial \theta} \quad \textbf{(partial M-step)}. \quad (22)$$

This, with a change of notation, is *incremental IL* as presented in section 2. To obtain *standard IL*, one employs a full E-step, followed by a partial M-step.

3.2 Generative Models

Having described the general process for minimizing the NLL, we can now proceed with modeling $p_\theta(x, z)$.

3.2.1 *PCNs of Rao & Ballard.* Here we derive the model of Rao & Ballard, i.e., PC with two layers. First factorize the generative model as:

$$p_\theta(x, z) = p(x|z)p(z). \quad (23)$$

To obtain the original results of Rao & Ballard, one assumes that both distributions on the right-hand side may be well-approximated by Gaussians. Hence for $p(x|z)$ we take

$$p(x|z) = \mathcal{N}(x; \mu_x, \Sigma_x) = \frac{1}{\sqrt{(2\pi)^{n_x} \det \Sigma_x}} \exp\left(-\frac{1}{2}(x - \mu_x)^T (\Sigma_x)^{-1} (x - \mu_x)\right), \quad (24)$$

and likewise for the prior, $p(z) = \mathcal{N}(z; \mu_z, \Sigma_z)$. Furthermore, take $\mu_x = f(W_x z)$ and $\mu_z = f(W_z z_p)$ with f, W_x, W_z defined as in section 2, and z_p a parameter for the prior (either fixed or learnable). $\Sigma_x \in \mathbb{R}^{n_x^2}, \Sigma_z \in \mathbb{R}^{n_z^2}$ are covariance matrices. Thus, $\theta = \{W_x, W_z, \Sigma_x, \Sigma_z\}$ are the parameters that define the generative model. For convenience, we also define the errors $\epsilon_x = x - \mu_x$ and $\epsilon_z = z - \mu_z$ as in section 2. The model is illustrated schematically in fig. 11.

With the decomposition (23), the energy (20) is

$$\begin{aligned} E(x, z) &= -\ln p(x|z) - \ln p(z) \\ &= \frac{1}{2} \left((\epsilon_x)^T (\Sigma_x)^{-1} \epsilon_x + (\epsilon_z)^T (\Sigma_z)^{-1} \epsilon_z + \ln [\det \Sigma_x \det \Sigma_z] \right) + \text{const.}, \end{aligned} \quad (25)$$

where on the second line we have inserted the Gaussian ansätze (24), the prior, and the constant – which is irrelevant to the optimization problem – is $\frac{1}{2}(n_x + n_z) \ln 2\pi$. Choosing diagonal bases so that $\Sigma = \sigma^2 I$, and disregarding the constant

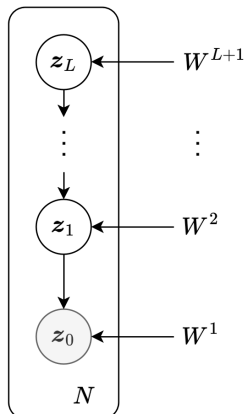


Fig. 12. **Graphical model for multi-layer PCNs**, with $\Sigma^\ell = I$. This defines the factorization of the observed variable (here z^0) and latent variables (z^ℓ), cf. (27). $\theta = \{W^\ell\}_{\ell=0}^{L+1}$ is shown as the set of deterministic parameters, and a plate labeled with N representing N nodes for the datapoints.

and the factor of 1/2, we have

$$E(\mathbf{x}, \mathbf{z}) = \frac{1}{\sigma_x^2} (\epsilon_x)^2 + \frac{1}{\sigma_z^2} (\epsilon_z)^2, \quad (26)$$

which is the energy function used by Rao & Ballard [75] (with variances taken as constants). With a model for E in hand, we can now apply EM, cf. (18) and (19).

3.2.2 Multi-layer PC. We now extend the previous section to a model with L layers (vectors) of latent variables $\{z^\ell\}_{\ell=1}^L$ in a hierarchical structure. It is convenient to label the observed variables \mathbf{x} as $\mathbf{x} = z^0 \in \mathbb{R}^{n_\ell}$. Thus our generative model is $p_\theta(\mathbf{x}, \{z^\ell\}) = p_\theta(z^0, \dots, z^L) = p_\theta(\{z^\ell\})$. The hierarchical structure then translates to the statement that each layer is conditionally independent given the layer above, i.e.,

$$p_\theta(\{z^\ell\}) = p_\theta(z^L) \prod_{\ell=0}^{L-1} p_\theta(z^\ell | z^{\ell+1}), \quad (27)$$

so that the energy becomes

$$\begin{aligned} E(\{z^\ell\}) &= -\ln p_\theta(\{z^\ell\}) \\ &= -\ln p_\theta(z^L) - \sum_{\ell=0}^{L-1} \ln p_\theta(z^\ell | z^{\ell+1}). \end{aligned} \quad (28)$$

As in the simple model above, we assume a multidimensional Gaussian for the conditional distribution of each layer, as well as for the prior:¹³

$$\begin{aligned} p_\theta(z^\ell | z^{\ell+1}) &= \mathcal{N}(z^\ell; \boldsymbol{\mu}^\ell, \Sigma^\ell) \\ p(z^L) &= \mathcal{N}(z^L; \boldsymbol{\mu}^L, \Sigma^L) \end{aligned} \quad (29)$$

with mean $\boldsymbol{\mu}^\ell = f(W^{\ell+1} z^{\ell+1})$ and covariance matrix $\Sigma^\ell \in \mathbb{R}^{n_\ell \times n_\ell}$, where $W^\ell \in \mathbb{R}^{n_\ell \times n_{\ell+1}}$ and $\boldsymbol{\mu}^L = f(W^{L+1} z_p)$. These parameters, $\theta = \{W^\ell, \Sigma^\ell\}_{\ell=0}^{L+1}$, define the generative model, which is illustrated in fig. 12. As before, we define the errors

¹³This is a reasonable assumption for traditional (fully-connected, feedforward) ANNs with large layer widths, $n_\ell \sim n \gg 1$, which becomes exact in the so-called large-width limit $n \mapsto \infty$, due to the central limit theorem. However, non-Gaussianities appear at finite width (see, e.g., [32, 77] for theoretical treatments), and it is unclear how realistic this assumption is in more general networks involving intralayer or feedback connections.

$\epsilon^\ell = \mathbf{z}^\ell - \boldsymbol{\mu}^\ell$. We then have

$$-\ln p(\mathbf{z}^\ell | \mathbf{z}^{\ell+1}) = \frac{1}{2} \left((\epsilon^\ell)^T (\Sigma^\ell)^{-1} \epsilon^\ell + \ln \det \Sigma^\ell + n_\ell \ln 2\pi \right) \quad (30)$$

such that E becomes

$$E(\{\mathbf{z}^\ell\}) = \frac{1}{2} \sum_{\ell=0}^L \left((\epsilon^\ell)^T (\Sigma^\ell)^{-1} \epsilon^\ell + \ln \det \Sigma^\ell \right) + \text{const}, \quad (31)$$

where the constant is $\sum_{\ell=0}^L n_\ell \ln 2\pi$. Dropping this, and choosing a diagonal basis so that $\Sigma^\ell = I$, we obtain

$$E(\{\mathbf{z}^\ell\}) = \frac{1}{2} \sum_{\ell=0}^L (\epsilon^\ell)^2 \quad (32)$$

which is the energy of Section 2; cf. also (26). Applying EM to this then yields IL as presented in section 2 (replacing \mathbf{z}^ℓ by $\mathbf{a}^{\ell 14}$).

3.3 Learning in PCNs Revisited

3.3.1 Discriminative and Generative PCNs. At this point we can provide a number of interesting interpretations of earlier sections. Notice that in the derivation above, the model had observed variables at layer $\ell = 0$. This corresponds to *generative PCN*, as discussed in section 2.5. If trained in supervised mode, we can understand the clamping of the label $\mathbf{y}^{(n)}$ to the final layer \mathbf{z}^p as follows: $\mathbf{y}^{(n)}$ becomes a parameter of the prior (e.g. its mean). If trained in unsupervised mode, it is treated just like the other hidden variables. Interestingly then, for a *discriminative PCN*, we see that the clamped data $\mathbf{x}^{(n)}$ is a parameter for the prior, and the label is now the observed variable. This is shown in table 6.

Table 6. Overview of learning modes in the probabilistic perspective of PCNs.

		Generative PCN		Discriminative PCN
		Unsupervised learning	Supervised learning	Supervised learning
\mathbf{z}^L	Prior parameter	-	Label $\mathbf{y}^{(n)}$	Data $\mathbf{x}^{(n)}$
\mathbf{z}^0	Observed variable	Data $\mathbf{x}^{(n)}$	Data $\mathbf{x}^{(n)}$	Label $\mathbf{y}^{(n)}$

3.3.2 Precision Matrices. In the context of predictive coding, the covariance matrices Σ^ℓ are often interpreted as the uncertainty at each layer around the mean $\boldsymbol{\mu}^\ell$, with their inverse $(\Sigma^\ell)^{-1} =: \Pi^\ell$ sometimes called *precision matrices* [25, 53, 58]. Within neuroscience and psychology, they have been used in a wide range of models [56], where it has been suggested that they implement a type of attention [21]. By up-weighting the error, increasing the precision of a variable would serve as a form of gain modulation. From the ML perspective, instead of setting them to identity matrices, one can add minimization of E w.r.t. Π^ℓ as an additional part of the M-step, seeing them simply as additional parameters of the generative model. However, their practical utility remains unclear, with varying results. In particular, [62] do not find advantages of additionally learning for generative modeling tasks, while [65] do appear to find some benefit, suggesting they act as a type of lateral modulation that induces a useful form of sparsity in the model. Comparisons with VAEs are made in [73], with a different theoretical interpretation by [58] (cf. section 4 for further discussion).

¹⁴Following typical ML notation, we use \mathbf{z} for latent variables in the context of graphical models, and \mathbf{a} for activation neurons in the neural network context.

3.4 Connections to Other Latent Variable Models

PCNs share various properties with other probabilistic models in machine learning. We briefly discuss some of these connections here, leaving more extensive comparisons (e.g., on training methods, sampling) for future work.

3.4.1 Linear Factor Models. With f as a linear function, the two-layer PCN model discussed above is equivalent to a *linear factor model*. This is illustrated in fig. 13. Specifically, if we take $\mu_z = \mathbf{0}$, $\Sigma_z = I$, and $\Sigma_x = \text{diag } \sigma^2$ with $\sigma^2 = [\sigma_1^2, \sigma_2^2, \dots, \sigma_n^2]^T$, then we obtain exactly *factor analysis*. If additionally take $\Sigma_x = \sigma^2 I$, i.e. the variances σ_i^2 are all equal to each other, we obtain *probabilistic PCA* [31]. Like in PCNs, parameters in this model can be learned using the EM algorithm [7].

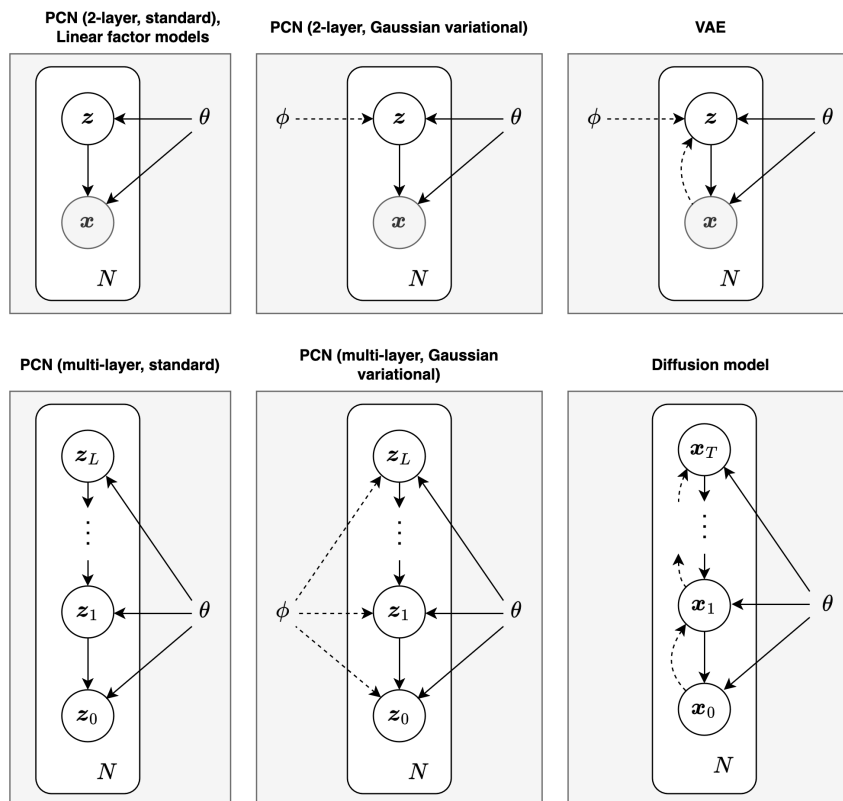


Fig. 13. **Graphical model comparison of PCNs and other probabilistic models**, with θ model parameters and ϕ variational parameters (cf. appendix A). Standard PCNs (left column) use MAP inference of the latent variables during the E-step, without variational parameters. Using a Gaussian variational (middle column) adds the mean and variance of the variational as parameters ϕ which may additionally be varied, shown by dotted lines. This is similar to ϕ in a VAE (top right). VAEs differ from PCNs in that their variational posterior is conditioned explicitly on \mathbf{x} (i.e. $q(\mathbf{z}|\mathbf{x})$ in VAEs vs. $q(\mathbf{z})$ in PCNs). Diffusion models similarly use a conditioned variational, and are similar to hierarchical VAEs [74]. However, diffusion models do not use variational parameters ϕ , and their latent variables have the same dimensionality as the observed variable, hence their use of \mathbf{x} instead of \mathbf{z} .

3.4.2 VAEs and Diffusion Models. VAEs share many properties with PCNs, as discussed in [52, 53, 62, 73]. They make use of a similar graphical model as two-layer PCNs (and linear factor models). VAEs are trained using variational free

energy as an upper bound for the NLL (cf. appendix A). While they use different optimization techniques, these can be seen as design choices for solving the same inference problem [53]. A number of key differences can be identified. First, the conditional $p(\mathbf{x}|z)$ is parametrized by a linear function, followed by a nonlinearity (i.e. $f(W^z z)$). In contrast, VAEs use a deep neural network (trained with BP). Moreover, in the variational inference perspective, whereas PCNs use a variational posterior of the form $q(z)$, VAEs use $q_\phi(z|\mathbf{x})$, i.e. with an explicit conditioning on data (visualized by dotted lines in fig. 13). This is parameterized by a separate neural network through parameters ϕ , which are learned jointly with θ using BP. For further comparisons, see [52, 53].

Adding multiple layers to VAEs results in *hierarchical VAEs*, which can similarly be compared to multi-layer PCNs. *Diffusion models* are also shown in fig. 13, which share (most of) their graphical structure with hierarchical VAEs. Like VAEs, diffusion models factorize the variational posterior using conditional distributions, i.e. $q(\mathbf{x}^\ell|\mathbf{x}^{\ell+1})$, but this is not parametrized by separate parameters ϕ . I.e. the variational model is not learned, but fixed.

In terms of performance, comparisons between multi-layer PCNs and (non-hierarchical) VAEs have been studied by [62, 65, 73, 111]. PCNs seem to compare favourably, with similar or improved results on several metrics, especially in the most recent work of [111]. At the same time (similar to the picture that emerged for PCNs used for supervised learning), PCNs seem to be more computationally costly to train, though again relatively little work has been done on training optimization in comparison to that for VAEs. Comparisons with hierarchical VAEs and diffusion models have not yet been done to the authors' knowledge.

3.4.3 Energy-Based Models (EBMs). PCNs are often cited to belong to the class of EBMs [57, 58, 94]. However, in these works the term 'EBM' is used in a different way than is typical in ML. The typical use of EBM [45, 98] is based on the observation that any probability distribution function can be parametrized by:

$$p_\theta(\mathbf{x}) = \frac{\exp(-E_\theta(\mathbf{x}))}{Z(\theta)}, \quad (33)$$

where $E_\theta(\mathbf{x})$ is the *energy* function, and $Z(\theta)$ is the partition function, i.e., the sum of all possible states. This use comes from physics where (33) is called a Boltzmann distribution, corresponding to a system at thermal equilibrium described by a canonical ensemble. The prototypical example of EBMs are Boltzmann machines, which have $E_\theta(\mathbf{x}) = -\frac{1}{2}\mathbf{x}^T W \mathbf{x}$ [2, 50].

In contrast, in [57, 58, 94] an EBM is instead defined through (21) and (22) [57, 58, 94]. This definition has also been used by [88], and encompasses continuous Hopfield networks and networks trainable by Equilibrium Propagation. Indeed, PCNs have much in common with these techniques, cf. [57] and section 4.

Regarding EBMs as defined by (33), comparisons of PCNs with this class of models has not yet been done to the authors' knowledge. We briefly mention some differences here, comparing to Boltzmann machines.¹⁵ If one includes latent variables z , one may write $p_\theta(\mathbf{x}) = \sum_z p_\theta(\mathbf{x}, z)$ (with a sum instead of an integral because nodes in Boltzmann machines are typically discrete), with [50]:

$$p(\mathbf{x}, z) = \frac{\exp(-E_\theta(\mathbf{x}, z))}{Z(\theta)}. \quad (34)$$

Now, observe that the generative model of PCNs, by definition of E (cf. (20)), can be written as $p_\theta(\mathbf{x}, z) = \exp(-E_\theta(\mathbf{x}, z))$, which is similar to (34). However, note that E in this equation is not a proper 'energy' as in (33) due to the lack of

¹⁵Boltzmann machines are characterized by all-to-all connectivity between nodes. Another important class of models is obtained by restricting the weight matrix to only include connections between \mathbf{x} and z , whereupon one obtains restricted Boltzmann machines (RBMs), which can be stacked to obtain a hierarchical structure with interesting Bayesian interpretations [31].

normalization in Z . Comparing EBMs to PCNs, one may first observe that E is of course different. Another difference is that PCNs minimize $-\ln p_{\theta}(\mathbf{x}, \mathbf{z})$, whereas EBMs typically minimize the NLL itself – not by using EM, but taking derivatives of the NLL w.r.t. model parameters, calculated using MCMC techniques, e.g. Gibbs sampling [31]. Clarifying these differences further could be an interesting direction for future work, further bringing PC and ML closer together.

4 PCNs and Inference Learning

This section discusses IL in detail, which has been the focus of much of the recent literature – particularly on the connection between IL and BP. Various ways of modifying IL have been introduced to approximate or replicate BP’s weight updates. More recent works however, instead consider IL in its ‘natural regime’ – meaning without modifications as presented in section 2. It has also become understood that PCNs/IL share properties with other algorithms, like target propagation [58] and trust region methods [37]. We review these below. In general, much is still unclear about the properties of PCNs and IL. In particular, the properties of IL in generative PCNs and PC graphs remain underexplored.

4.1 Relation to BP

As far as we are aware, the first use of PC applied to an ML task was [104]. They showed, under certain strict conditions, that the weight updates of IL on discriminative PCNs approximates the parameter updates of BP in FNNs. Subsequently, this result was shown to generalize – again with strict conditions – to any computational graph (a decomposition of complex functions such as DL architectures, e.g. FNNs, CNNs and RNNs, into elementary functions) [56, 78]. Using a different method, it was shown that a variation of PC, called Z-IL, gives the *exact* weight updates of BP on any computational graph [85, 86, 93]. The reason this works is that Z-IL uses a highly specific number of inference steps that matches the number of layers, and updates weights of different layers at very specific steps during inference. Another requirement is that the ‘feedforward pass’ initialization of hidden nodes is done (cf. section 2.2.2). Alg. 4 (appendix B.4) shows pseudocode for Z-IL.

Since it has been known that other algorithms (Equilibrium Propagation [88], Contrastive Hebbian Learning [105]) also approximate BP, work by [57] showed that these various approximations can be understood as a consequence of certain properties of energy-based models (EBMs), as defined by (21) and (22) (cf. section 3.4.3). A practical limitation of these works is that the various approximations and variants of PC always remain slower than the (highly optimized) BP [110]. As such, they do not provide a clear argument for using e.g. Z-IL in practical applications.

Another interesting theoretical connection found by [58] is that PC can be understood to *interpolate* between BP and a third algorithm for training neural networks, called *target propagation* (TP) [46]. This algorithm propagates *target activations* (not errors) to the hidden layers of the network, followed by updating weights of each layer to move closer to the target activation. The authors show that if a PCN is trained *with only labels clamped*, the activities converge to the targets computed by TP. At the same time (as was shown in section 2), *with only data clamped*, the activations computed with IL are equal to feedforward ANN activations. As such, the equilibrium of IL’s inference phase with *both* data and labels clamped can be interpreted as an average of the feedforward pass values of the network, and the local targets computed by TP. Furthermore, they observe that *precision weights* $\Pi^{\ell} = (\Sigma^{\ell})^{-1}$ provide a means to change the relative weighting of the feedforward and feedback influences on the network dynamics (cf. section 3.3.2).

4.2 IL in its Natural Regime

Following insights from the aforementioned references, recent works have instead started to consider the ‘natural’ regime of IL as presented in section 2, without modifications. So far, no comprehensive account of the properties of IL exists, so we review the somewhat disparate theoretical results in the literature.

Although most works study properties of the learning algorithm as a whole, the work of [23] showed a useful result concerning the inference phase. Using a dynamical systems perspective, they formally prove that the inference phase (during training and testing) converges only when γ and α (the inference and learning rate, respectively) are smaller than 1. This is always done in practice, but [23] gave theoretical assurance that this is indeed the case. Then, the first contribution to a theory for why IL sometimes performs better than BP was provided by [94], which according to the authors lies in *reduced weight interference*. ‘Catastrophic interference’ is a well-known pathology of BP to abruptly and drastically forget previously learned information upon learning new information [42]. According to [94], this is reduced in IL, since before weight update, activation nodes are changed to a new state which is closer to what the network should ideally predict to obtain the observed outcome. They call this mechanism *prospective configuration*, since IL is ‘prospective’ in the sense that it can foresee side effects of weight modifications, leading to decreased weight interference. This helps to explain improved empirical results seen in continual learning tasks (which are a challenge precisely due to this interference), online learning, and the generally observed faster convergence.

In a parallel line of work, [6] showed both theoretically and empirically that IL approximates *implicit SGD*, which provides increased stability across learning rates. The authors also develop a variant of PC in which updates become equal to implicit SGD, further improving the stability. This is extended in [5], where the authors observe that implicit SGD is sensitive to second-order information, i.e. the second derivative of the loss landscape (its curvature). This can speed up convergence. As such, when IL approximates implicit SGD, IL uses this information, which explains the faster convergence also observed by [94].

This connects to [37], which related IL to *trust region (TR) methods*. These are a well-known method in optimization, which can be contrasted with line-search methods such as gradient descent [107]. Such methods define a neighborhood around the current best solution as a *trust region* in each step, which is changed adaptively in addition to the step direction [107]. The authors show [37] that IL’s inference phase of PC can be understood as solving a TR problem on the BP loss, using a trust region defined by a second derivative of the energy. By using this second-order information, trust region methods are well-known to be better at escaping saddle points. Indeed, [37] show that these properties transfer to IL, thus drawing a similar conclusion as [5]. They prove on toy problems that IL escapes saddle points faster, and provide evidence that this happens in larger networks by training deep chains, where IL converges significantly faster than BP. These results help to explain the empirical results showing faster convergence of PC compared to BP (cf. section 2.3.5).

Theoretical results of [58] are concerned with the convergence in PCN’s energy landscape. The authors showed that that when activity nodes are initialized with the so-called ‘energy gradient bound’, IL converges to *the same extrema* in the loss as BP. This can be understood by writing PCN’s energy as a sum of two terms $E = \mathcal{L} + \tilde{E}$, where $\mathcal{L} = (\epsilon^L)^2$ is the energy of the last layer, equal to the BP MSE loss, and $\tilde{E} = \sum_{\ell=1}^{L-1} (\epsilon^\ell)^2$ is the residual energy. Now, during inference, minimizing E is guaranteed to minimize \mathcal{L} if the following holds that (cf. [58] for a derivation) $-\left(\frac{\partial \mathcal{L}}{\partial \mathbf{a}^\ell}\right)^\top \frac{\partial \tilde{E}}{\partial \mathbf{a}^\ell} \leq \left\| \frac{\partial \mathcal{L}}{\partial \mathbf{a}^\ell} \right\|^2$, which implies that the gradient of \mathcal{L} is greater than the negative gradient of the residual energy. At the beginning of inference this always holds when using feedforward-pass initialization of hidden activities, since then $\partial \tilde{E} / \partial \mathbf{a}^\ell = 0$. Indeed, [58] show that this keeps being true also in practice throughout inference, with a sufficiently small learning

rate (up to 0.1, which is 2-3 orders of magnitude larger than step sizes typically used in practice). If the learning step is additionally written as a minimization of \mathcal{L} , [58] show that IL will lead to the same minima as BP, even though the weight updates of BP and IL are different. This helps explain the fact that in practice, performance of IL very closely matches BP [6, 78, 87, 94, 104]. Consequently, deep PCNs could potentially achieve the same generalization performance as BP while maintaining their advantages.

This result seems to be contradicted in part by [24] however, which shows that use of activation functions with many zeros (such as ReLU) can be problematic for PCNs, since they can prevent convergence of learning. This result is interesting in light of [37] which highlights how ReLU does not show the same speed benefits as other activation functions. Interestingly, even for ANNs, more sophisticated treatments indicate that ReLU is a suboptimal choice of activation function due to the fact that the critical regime reduces to a single point in phase space [77]. In general, these works show how although PCNs and ANNs are similar in many respects, one cannot rely completely on existing knowledge about BP-based frameworks for predicting properties of PCNs.

4.3 Improving Performance

As was mentioned, the notion of doing EM incrementally was a recent successful approach to improving the efficiency of IL, improving the time complexity of a weight update by a factor T . A second proposal for modifying IL to improve its complexity comes from [5], who suggest that the inference phase includes a delay in the computation of errors, where updates in earlier layers are zero at the beginning of inference. They suggest changing the inference to not update layers in parallel, but sequentially from layer L to layer 0, thus proposing ‘sequential inference’. The authors observe that this decreases the number of time-steps required per weight update without sacrificing performance. However, we remark that this change effectively updates lower layers faster than would otherwise happen, and is thus a change to (11). It is also reminiscent of Z-IL as discussed above, making IL closer to BP in some sense. As such, it is unclear whether this preserves the advantages of IL observed in other works. In the same work, the authors build on the observation of [6] that IL sometimes converges to poor local minima when trained with SGD. They suggest this may be caused by increasingly small weight updates in lower layers. They suggest an optimizer created for IL specifically (dubbed Matrix Update Equalization (MQ)-optimizer) that requires less memory than Adam, and similarly appears to avoid poor local minima, with promising initial results.

5 Conclusion

Despite the remarkable successes of deep learning witnessed in recent years, biological learning is still superior to machine learning (ML) in many key respects, such as energy and data efficiency [108]. Whereas the most successful deep learning approaches rely on backpropagation (BP) as a training algorithm, recent work [94] identified the learning mechanisms in *predictive coding networks* (PCNs), trained with inference learning (IL), to provide an improved model for many features of biological learning.

Research on PCNs has recently witnessed a burst in activity. These networks build on the neuroscientific theory of predictive coding (PC), thus exemplifying recent calls for renewed emphasis on neuroscience-inspired methods to artificial intelligence, called *NeuroAI* [108]. PCNs entail a flexible framework for ML that goes beyond traditional (BP-trained) artificial neural networks (ANNs). Despite the recent burst in activity, a comprehensive and mathematically oriented introduction aimed at machine learning practitioners has been lacking, which this tutorial has attempted to provide.

This work has discussed three complementary perspectives on PCNs (cf. fig. 3):

- (1) a model that generalizes the structure of ANNs (the most recent notion, due to [83]);
- (2) a probabilistic latent variable model for unsupervised learning (its inception [75]);
- (3) a learning algorithm (IL) that can be compared to BP (the most common conception in the recent literature, as for example in [94]).

The first perspective, PCNs as a generalized ANN, is justified by the fact that mathematically, the structure of PCNs forms a superset of traditional ANNs (a fact that follows from earlier work, but has not been pointed out as a general conception of PCNs). Thus, we expect PCNs share the appealing property of being universal function approximators, while also providing a broader, more general framework as a neural network. Namely, a simple choice of direction gives networks appropriate not only for supervised learning and classification, but also unsupervised learning in generative models. Next to this, the generalization of PCNs to *arbitrary* graphs (PC graphs) [83] means a large new set of structures untrainable by BP can be studied theoretically and empirically. Given the topological nature of several advances in machine learning in the past (such as residual networks [109] and the notion of *depth* itself [74]), this suggests an interesting avenue for further work.

The second perspective, PCN as probabilistic latent variable model, provides a principled derivation of equations that underlie PCNs. In addition, it brings to light the mentioned connections to other ML algorithms. PCNs share several properties both with classic methods such as factor analysis, but also to modern methods such as diffusion models – associated with the remarkable success of generative AI witnessed in recent years [74]. In general, PCNs’ probabilistic nature and these various connections also suggest they could potentially be developed further as a method for *Bayesian deep learning*, which aim to reliably assess uncertainties and incorporate existing knowledge [70, 101].

The third perspective has been the focus of most of the recent literature on PCNs [57, 78, 104]. Existing implementations of IL are still inefficient compared to BP, which has prevented adoption of PCNs for practical applications, but recent work has taken important steps towards improving efficiency, showing that IL no longer scales with the depth of the network (i.e. it is an order L network depth faster per weight update), if sufficient parallelization is achieved [87]. The reason for this is IL’s local computations, which could bring advantages as deep networks keep scaling up, or on neuromorphic hardware. Barring the issue of efficiency, IL demonstrates favorable properties which call for further investigation. In particular, decreased weight interference [94] and sensitivity to second-order information [6, 37], which can lead to faster convergence and increased performance on certain learning tasks (e.g. continual learning and adaptation to changing environments). To what extent these results generalize and scale remains to be studied, but theoretical results suggest that IL should perform at least as well as BP in terms of generalization, potentially opening the door to additional advantages [58].

Finally, we remark that although we have so far refrained from discussing aspects of PC related to biology, psychology, and philosophy, we argue that a ML/computer science perspective is useful for these fields too, since formal detail can help clarify PC’s computational properties. This tutorial can be used to review the mathematics used in some of the more speculative works on PC in these domains.

In sum, this tutorial offers a formal overview of PCNs, complementing existing surveys with a detailed mathematical introduction and connections to other ML methods. It clarifies and structures various perspectives, making it an accessible starting point for researchers. As such, it can aid in accelerating future work in the emerging field of NeuroAI.

Acknowledgments

B.E.v.Z. and E.L.v.d.B. thank our partners, members from the HONDA project between the Honda Research Institute in Japan and Utrecht University in the Netherlands, for supporting this research. The funders had no role in study design, data collection and analysis, decision to publish or preparation of the manuscript. B.E.v.Z. thanks Lukas Arts and Mathijs Langezaal for helpful discussions and feedback.

References

- [1] 2024. The new NeuroAI. *Nature Machine Intelligence* 6, 3 (March 2024), 245–245. <https://doi.org/10.1038/s42256-024-00826-6>
- [2] David H. Ackley, Geoffrey E. Hinton, and Terrence J. Sejnowski. 1985. A learning algorithm for boltzmann machines. *Cognitive Science* 9, 1 (Jan. 1985), 147–169. [https://doi.org/10.1016/S0364-0213\(85\)80012-4](https://doi.org/10.1016/S0364-0213(85)80012-4)
- [3] Andrea Alamia, Milad Mozafari, Bhavin Choksi, and Rufin VanRullen. 2023. On the role of feedback in image recognition under noise and adversarial attacks: A predictive coding perspective. *Neural Networks* 157 (Jan. 2023), 280–287. <https://doi.org/10.1016/j.neunet.2022.10.020>
- [4] Nicholas Alonso. 2023. *An Energy-based Approach to Learning and Memory in Artificial Neural Networks*. Ph.D. Thesis. UC Irvine.
- [5] Nicholas Alonso, Jeffrey Krichmar, and Emre Neftci. 2024. Understanding and Improving Optimization in Predictive Coding Networks. *Proceedings of the AAAI Conference on Artificial Intelligence* 38, 10 (March 2024), 10812–10820. <https://doi.org/10.1609/aaai.v38i10.28954>
- [6] Nick Alonso, Beren Millidge, Jeffrey Krichmar, and Emre Neftci. 2022. A Theoretical Framework for Inference Learning. *Advances in Neural Information Processing Systems* 35 (Dec. 2022), 37335–37348. <https://doi.org/10.48550/arXiv.2206.00164>
- [7] Christopher M. Bishop. 2006. *Pattern Recognition and Machine Learning (Information Science and Statistics)*. Springer-Verlag, Berlin, Heidelberg.
- [8] Rafal Bogacz. 2017. A tutorial on the free-energy framework for modelling perception and learning. *Journal of Mathematical Psychology* 76 (Feb. 2017), 198–211. <https://doi.org/10.1016/j.jmp.2015.11.003>
- [9] Victor Boutin, Aimen Zerroug, Minju Jung, and Thomas Serre. 2020. Iterative VAE as a predictive brain model for out-of-distribution generalization. In *NeurIPS 2020 Workshop SVRHM*. <https://openreview.net/forum?id=jE6SIVTOFPV>
- [10] Christopher L. Buckley, Chang Sub Kim, Simon McGregor, and Anil K. Seth. 2017. The free energy principle for action and perception: A mathematical review. *Journal of Mathematical Psychology* 81 (Dec. 2017), 55–79. <https://doi.org/10.1016/j.jmp.2017.09.004>
- [11] Aleksandar Bukva, Jurriaan de Gier, Kevin T. Grosvenor, Ro Jefferson, Koenraad Schalm, and Eliot Schwander. 2023. Criticality versus uniformity in deep neural networks. (April 2023). arXiv:2304.04784. Retrieved from <https://arxiv.org/abs/2304.04784>.
- [12] Billy Byiringiro, Tommaso Salvatori, and Thomas Lukasiewicz. 2022. Robust Graph Representation Learning via Predictive Coding. arXiv:2212.04656. Retrieved from <https://arxiv.org/abs/2212.04656>.
- [13] Charlotte Caucheteux, Alexandre Gramfort, and Jean-Rémi King. 2023. Evidence of a predictive coding hierarchy in the human brain listening to speech. *Nature Human Behaviour* 7, 3 (March 2023), 430–441. <https://doi.org/10.1038/s41562-022-01516-2>
- [14] Rakesh Chalasani and Jose C. Principe. 2013. Deep Predictive Coding Networks. arXiv:1301.3541. Retrieved from <https://arxiv.org/abs/1301.3541>.
- [15] Bhavin Choksi, Milad Mozafari, Callum Biggs O’ May, B. ADOR, Andrea Alamia, and Rufin VanRullen. 2021. Predify: Augmenting deep neural networks with brain-inspired predictive coding dynamics. In *Advances in Neural Information Processing Systems*, Vol. 34. 14069–14083. <https://doi.org/10.5555/3540261.3541339>
- [16] Bhavin Choksi, Milad Mozafari, Callum Biggs O’May, B. Ador, Andrea Alamia, and Rufin VanRullen. 2020. Brain-inspired predictive coding dynamics improve the robustness of deep neural networks. In *NeurIPS 2020 Workshop SVRHM*. <https://openreview.net/forum?id=q1o2mWaOssG>
- [17] Andy Clark. 2016. *Surfing Uncertainty: Prediction, Action, and the Embodied Mind*. Oxford University Press.
- [18] P. Dayan, G. E. Hinton, R. M. Neal, and R. S. Zemel. 1995. The Helmholtz machine. *Neural Computation* 7, 5 (Sept. 1995), 889–904. <https://doi.org/10.1162/neco.1995.7.5.889>
- [19] A. P. Dempster, N. M. Laird, and D. B. Rubin. 1977. Maximum Likelihood from Incomplete Data via the EM Algorithm. *Journal of the Royal Statistical Society. Series B (Methodological)* 39, 1 (1977), 1–38. <https://doi.org/10.1111/j.2517-6161.1977.tb01600.x>
- [20] Grégory Faye, Guilhem Foulhé, and Rufin VanRullen. 2023. Mathematical Derivation of Wave Propagation Properties in Hierarchical Neural Networks with Predictive Coding Feedback Dynamics. *Bulletin of Mathematical Biology* 85, 9 (July 2023), 80. <https://doi.org/10.1007/s11538-023-01186-9>
- [21] Harriet Feldman and Karl J. Friston. 2010. Attention, Uncertainty, and Free-Energy. *Frontiers in Human Neuroscience* 4 (Dec. 2010), 215. <https://doi.org/10.3389/fnhum.2010.00215>
- [22] Linda Ficco, Lorenzo Mancuso, Jordi Manuella, Alessia Teneggi, Donato Liloia, Sergio Duca, Tommaso Costa, Gyula Zoltán Kovacs, and Franco Cauda. 2021. Disentangling predictive processing in the brain: a meta-analytic study in favour of a predictive network. *Scientific Reports* 11, 1 (Aug. 2021), 16258. <https://doi.org/10.1038/s41598-021-95603-5>
- [23] Simon Frieder and Thomas Lukasiewicz. 2022. (Non-)Convergence Results for Predictive Coding Networks. In *Proceedings of the 39th International Conference on Machine Learning (Proceedings of Machine Learning Research, Vol. 162)*, Kamalika Chaudhuri, Stefanie Jegelka, Le Song, Csaba Szepesvari, Gang Niu, and Sivan Sabato (Eds.). PMLR, 6793–6810.

- [24] Simon Frieder, Luca Pinchetti, and Thomas Lukasiewicz. 2024. Bad Minima of Predictive Coding Energy Functions. In *The Second Tiny Papers Track at ICLR 2024*. <https://openreview.net/forum?id=5Vc1ACZ8eC>
- [25] Karl Friston. 2003. Learning and inference in the brain. *Neural Networks* 16, 9 (Nov. 2003), 1325–1352. <https://doi.org/10.1016/j.neunet.2003.06.005>
- [26] Karl Friston. 2005. A theory of cortical responses. *Philosophical Transactions of the Royal Society of London. Series B, Biological Sciences* 360, 1456 (April 2005), 815–836. <https://doi.org/10.1098/rstb.2005.1622>
- [27] Karl Friston. 2008. Hierarchical Models in the Brain. *PLOS Computational Biology* 4, 11 (Nov. 2008), e1000211. <https://doi.org/10.1371/journal.pcbi.1000211>
- [28] Karl Friston. 2010. The free-energy principle: a unified brain theory? *Nature Reviews Neuroscience* 11, 2 (Feb. 2010), 127–138. <https://doi.org/10.1038/nrn2787>
- [29] Karl Friston, James Kilner, and Lee Harrison. 2006. A free energy principle for the brain. *Journal of Physiology-Paris* 100, 1 (July 2006), 70–87. <https://doi.org/10.1016/j.jphysparis.2006.10.001>
- [30] Siavash Golkar, Tiberiu Tesileanu, Yanis Bahroun, Anirvan Sengupta, and Dmitri Chklovskii. 2022. Constrained Predictive Coding as a Biologically Plausible Model of the Cortical Hierarchy. *Advances in Neural Information Processing Systems* 35 (Dec. 2022), 14155–14169. <https://doi.org/10.48550/arXiv.2210.15752>
- [31] Ian Goodfellow, Yoshua Bengio, and Aaron Courville. 2016. *Deep Learning*. MIT Press.
- [32] Kevin Grosvenor and Ro Jefferson. 2022. The edge of chaos: quantum field theory and deep neural networks. *SciPost Physics* 12, 3 (March 2022), 081. <https://doi.org/10.21468/SciPostPhys.12.3.081>
- [33] Kuan Han, Haiguang Wen, Yizhen Zhang, Di Fu, Eugenio Culurciello, and Zhongming Liu. 2018. Deep Predictive Coding Network with Local Recurrent Processing for Object Recognition. In *Advances in Neural Information Processing Systems*, Vol. 31. <https://doi.org/doi/10.5555/3327546.3327594>
- [34] Demis Hassabis, Dhharshan Kumaran, Christopher Summerfield, and Matthew Botvinick. 2017. Neuroscience-Inspired Artificial Intelligence. *Neuron* 95, 2 (July 2017), 245–258. <https://doi.org/10.1016/j.neuron.2017.06.011>
- [35] J J Hopfield. 1982. Neural networks and physical systems with emergent collective computational abilities. *Proceedings of the National Academy of Sciences* 79, 8 (April 1982), 2554–2558. <https://doi.org/10.1073/pnas.79.8.2554>
- [36] Yanping Huang and Rajesh P. N. Rao. 2011. Predictive coding. *Wiley Interdisciplinary Reviews. Cognitive Science* 2, 5 (Sept. 2011), 580–593. <https://doi.org/10.1002/wcs.142>
- [37] Francesco Innocenti, Ryan Singh, and Christopher Buckley. 2023. Understanding Predictive Coding as a Second-Order Trust-Region Method. In *ICML Workshop on Localized Learning (LLW)*. <https://openreview.net/forum?id=x7PUpFKZ8M>
- [38] Linxing Preston Jiang and Rajesh P. N. Rao. 2024. Dynamic predictive coding: A model of hierarchical sequence learning and prediction in the neocortex. *PLOS Computational Biology* 20, 2 (Feb. 2024), e1011801. <https://doi.org/10.1371/journal.pcbi.1011801>
- [39] Paul F. Kinghorn, Beren Millidge, and Christopher L. Buckley. 2023. Preventing Deterioration of Classification Accuracy in Predictive Coding Networks. In *Active Inference*. 1–15. https://doi.org/10.1007/978-3-031-28719-0_1
- [40] Diederik Kingma and Jimmy Ba. 2015. Adam: A Method for Stochastic Optimization. In *International Conference on Learning Representations (ICLR)*. <https://doi.org/10.48550/arXiv.1412.6980>
- [41] D. P. Kingma and M. Welling. 2014. Auto-Encoding Variational Bayes. In *International Conference on Learning Representations (ICLR)*. <https://dare.uva.nl/search?identifier=cf65ba0f-d88f-4a49-8ebd-3a7fce86edd7>
- [42] James Kirkpatrick, Razvan Pascanu, Neil Rabinowitz, Joel Veness, Guillaume Desjardins, Andrei A. Rusu, Kieran Milan, John Quan, Tiago Ramalho, Agnieszka Grabska-Barwinska, Demis Hassabis, Claudia Clopath, Dhharshan Kumaran, and Raia Hadsell. 2017. Overcoming catastrophic forgetting in neural networks. *Proceedings of the National Academy of Sciences* 114, 13 (March 2017), 3521–3526. <https://doi.org/10.1073/pnas.1611835114>
- [43] Dmitry Krotov and John J. Hopfield. 2016. Dense Associative Memory for Pattern Recognition. In *Advances in Neural Information Processing Systems*, Vol. 29. <https://doi.org/10.48550/arXiv.1606.01164>
- [44] Pablo Lanillos, Cristian Meo, Corrado Pezzato, A. Meera, M. Baioumy, Wataru Ohata, Alexander Tschantz, Beren Millidge, M. Wisse, C. Buckley, and J. Tani. 2021. Active Inference in Robotics and Artificial Agents: Survey and Challenges. arXiv:2112.01871. Retrieved from <https://arxiv.org/abs/2112.01871>.
- [45] Yann Lecun, Sumit Chopra, Raia Hadsell, Marc Aurelio Ranzato, and Fu Jie Huang. 2006. A tutorial on energy-based learning. In *Predicting structured data*, G. Bakir, T. Hofman, B. Scholkopf, A. Smola, and B. Taskar (Eds.). MIT Press.
- [46] Dong-Hyun Lee, Saizheng Zhang, Asja Fischer, and Yoshua Bengio. 2015. Difference Target Propagation. In *Machine Learning and Knowledge Discovery in Databases*. 498–515. https://doi.org/10.1007/978-3-319-23528-8_31
- [47] Tianjin Li, Mufeng Tang, and Rafal Bogacz. 2023. Modeling Recognition Memory with Predictive Coding and Hopfield Networks. In *Associative Memory & Hopfield Networks in 2023*. <https://openreview.net/forum?id=gzFuhvumGn>
- [48] William Lotter, Gabriel Kreiman, and David Cox. 2017. Deep Predictive Coding Networks for Video Prediction and Unsupervised Learning. In *International Conference on Learning Representations*. <https://openreview.net/forum?id=B1ewdt9xe>
- [49] D. J. C. MacKay. 2001. A Problem with Variational Free Energy Minimization. (2001).
- [50] David J. C. MacKay. 2003. *Information Theory, Inference, and Learning Algorithms*. Copyright Cambridge University Press.
- [51] Tom Macpherson, Anne Churchland, Terry Sejnowski, James DiCarlo, Yukiyasu Kamitani, Hidehiko Takahashi, and Takatoshi Hikida. 2021. Natural and Artificial Intelligence: A brief introduction to the interplay between AI and neuroscience research. *Neural Networks* 144 (Dec. 2021),

- 603–613. <https://doi.org/10.1016/j.neunet.2021.09.018>
- [52] Joseph Marino. 2019. Predictive Coding, Variational Autoencoders, and Biological Connections. In *Real Neurons & Hidden Units: Future directions at the intersection of neuroscience and artificial intelligence @ NeurIPS 2019*. <https://openreview.net/forum?id=SyeumQYUUH>
- [53] Joseph Marino. 2022. Predictive Coding, Variational Autoencoders, and Biological Connections. *Neural Computation* 34, 1 (Jan. 2022), 1–44. https://doi.org/10.1162/neco_a_01458
- [54] Pankaj Mehta, Marin Bukov, Ching-Hao Wang, Alexandre G. R. Day, Clint Richardson, Charles K. Fisher, and David J. Schwab. 2019. A high-bias, low-variance introduction to Machine Learning for physicists. *Physics Reports* 810 (May 2019), 1–124. <https://doi.org/10.1016/j.physrep.2019.03.001>
- [55] Beren Millidge. 2021. *Applications of the free energy principle to machine learning and neuroscience*. Ph.D. Thesis.
- [56] Beren Millidge, Anil Seth, and Christopher L. Buckley. 2022. Predictive Coding: a Theoretical and Experimental Review. arXiv:2107.12979. Retrieved from <https://arxiv.org/abs/2107.12979>.
- [57] Beren Millidge, Yuhang Song, Tommaso Salvatori, Thomas Lukasiewicz, and Rafal Bogacz. 2023. Backpropagation at the Infinitesimal Inference Limit of Energy-Based Models: Unifying Predictive Coding, Equilibrium Propagation, and Contrastive Hebbian Learning. In *The Eleventh International Conference on Learning Representations*. <https://openreview.net/forum?id=nIMifqu2EO>
- [58] Beren Millidge, Yuhang Song, Tommaso Salvatori, Thomas Lukasiewicz, and Rafal Bogacz. 2023. A Theoretical Framework for Inference and Learning in Predictive Coding Networks. In *The Eleventh International Conference on Learning Representations*. https://openreview.net/forum?id=ZCTvSF_uVM4
- [59] Beren Millidge, Mufeng Tang, Mahyar Osanlouy, Nicol S. Harper, and Rafal Bogacz. 2024. Predictive coding networks for temporal prediction. *PLOS Computational Biology* 20, 4 (April 2024), e1011183. <https://doi.org/10.1371/journal.pcbi.1011183>
- [60] Beren Millidge, Alexander Tschantz, and Christopher L. Buckley. 2022. Predictive Coding Approximates Backprop Along Arbitrary Computation Graphs. *Neural Computation* 34, 6 (May 2022), 1329–1368. https://doi.org/10.1162/neco_a_01497
- [61] Radford M. Neal and Geoffrey E. Hinton. 1998. A View of the EM Algorithm that Justifies Incremental, Sparse, and other Variants. In *Learning in Graphical Models*, Michael I. Jordan (Ed.). Dordrecht, 355–368.
- [62] André Ofner, Beren Millidge, and Sebastian Stober. 2022. Generalized Predictive Coding: Bayesian Inference in Static and Dynamic models. In *SVRHM 2022 Workshop @ NeurIPS*. https://openreview.net/forum?id=qaT_CByg1X5
- [63] Kayoko Okada, William Matchin, and Gregory Hickok. 2018. Neural evidence for predictive coding in auditory cortex during speech production. *Psychonomic Bulletin & Review* 25, 1 (Feb. 2018), 423–430. <https://doi.org/10.3758/s13423-017-1284-x>
- [64] Alexander Ororbia. 2023. Spiking neural predictive coding for continually learning from data streams. *Neurocomputing* 544 (Aug. 2023), 126292. <https://doi.org/10.1016/j.neucom.2023.126292>
- [65] Alexander Ororbia and Daniel Kifer. 2022. The neural coding framework for learning generative models. *Nature Communications* 13, 1 (April 2022), 2064. <https://doi.org/10.1038/s41467-022-29632-7>
- [66] Alexander Ororbia and Ankur Mali. 2023. Convolutional Neural Generative Coding: Scaling Predictive Coding to Natural Images. arXiv:2211.12047. Retrieved from <https://arxiv.org/abs/2211.12047>.
- [67] Alex Ororbia, Ankur Mali, C. Lee Giles, and Daniel Kifer. 2022. Lifelong Neural Predictive Coding: Learning Cumulatively Online without Forgetting. In *Advances in Neural Information Processing Systems*. <https://openreview.net/forum?id=ccYOWWNa5v2>
- [68] Alexander G. Ororbia and Ankur Mali. 2022. Backprop-Free Reinforcement Learning with Active Neural Generative Coding. *Proceedings of the AAAI Conference on Artificial Intelligence* 36, 1 (June 2022), 29–37. <https://doi.org/10.1609/aaai.v36i1.19876>
- [69] Zhaoyang Pang, Callum Biggs O’May, Bhavin Choksi, and Rufin VanRullen. 2021. Predictive coding feedback results in perceived illusory contours in a recurrent neural network. *Neural Networks* 144 (Dec. 2021), 164–175. <https://doi.org/10.1016/j.neunet.2021.08.024>
- [70] Theodore Papamarkou, Maria Skoularidou, Konstantina Palla, Laurence Aitchison, Julian Arbel, David Dunson, Maurizio Filippone, Vincent Fortuin, Philipp Hennig, José Miguel Hernández-Lobato, Aliaksandr Hubin, Alexander Immer, Theofanis Karaletsos, Mohammad Emtiyaz Khan, Agustinus Kristiadi, Yingzhen Li, Stephan Mandt, Christopher Nemeth, Michael A. Osborne, Tim G. J. Rudner, David Rügamer, Yee Whye Teh, Max Welling, Andrew Gordon Wilson, and Ruqi Zhang. 2024. Position: Bayesian Deep Learning is Needed in the Age of Large-Scale AI. In *Forty-first International Conference on Machine Learning*. <https://openreview.net/forum?id=PrmxFWI1Fr>
- [71] Thomas Parr, Giovanni Pezzulo, and Karl J. Friston. 2022. *Active Inference: The Free Energy Principle in Mind, Brain, and Behavior*. The MIT Press. <https://doi.org/10.7551/mitpress/12441.001.0001>
- [72] Adam Paszke, Sam Gross, Francisco Massa, Adam Lerer, James Bradbury, Gregory Chanan, Trevor Killeen, Zeming Lin, Natalia Gimelshein, Luca Antiga, Alban Desmaison, Andreas Köpf, Edward Yang, Zach DeVito, Martin Raison, Alykhan Tejani, Sasank Chilamkurthy, Benoit Steiner, Lu Fang, Junjie Bai, and Soumith Chintala. 2019. PyTorch: an imperative style, high-performance deep learning library. In *Proceedings of the 33rd International Conference on Neural Information Processing Systems*. Number 721. Curran Associates Inc., Red Hook, NY, USA, 8026–8037.
- [73] Luca Pinchetti, Tommaso Salvatori, Yordan Yordanov, Beren Millidge, Yuhang Song, and Thomas Lukasiewicz. 2022. Predictive Coding beyond Gaussian Distributions. In *Advances in Neural Information Processing Systems*. <https://openreview.net/forum?id=Ryy7tVvBUK>
- [74] Simon J. D. Prince. 2023. *Understanding Deep Learning*. The MIT Press. <http://udlbook.com>
- [75] Rajesh P. N. Rao and Dana H. Ballard. 1999. Predictive coding in the visual cortex: a functional interpretation of some extra-classical receptive-field effects. *Nature Neuroscience* 2, 1 (Jan. 1999), 79–87. <https://doi.org/10.1038/4580>
- [76] Jan Rathjens and Laurenz Wiskott. 2024. Classification and Reconstruction Processes in Deep Predictive Coding Networks: Antagonists or Allies? arXiv:2401.09237. Retrieved from <https://arxiv.org/abs/2401.09237>.

- [77] Daniel A. Roberts, Sho Yaida, and Boris Hanin. 2022. *The Principles of Deep Learning Theory*. Cambridge University Press.
- [78] Robert Rosenbaum. 2022. On the relationship between predictive coding and backpropagation. *PLOS ONE* 17, 3 (March 2022), e0266102. <https://doi.org/10.1371/journal.pone.0266102>
- [79] F. Rosenblatt. 1958. The perceptron: A probabilistic model for information storage and organization in the brain. *Psychological Review* 65, 6 (1958), 386–408. <https://doi.org/10.1037/h0042519>
- [80] Tommaso Salvatori. 2022. *Learning and memorization via predictive coding*. Ph.D. Thesis. University of Oxford.
- [81] Tommaso Salvatori, Ankur Mali, Christopher L. Buckley, Thomas Lukasiewicz, Rajesh P. N. Rao, Karl Friston, and Alexander Ororbia. 2023. Brain-Inspired Computational Intelligence via Predictive Coding. arXiv:2308.07870. Retrieved from <https://arxiv.org/abs/2308.07870>.
- [82] Tommaso Salvatori, Luca Pinchetti, Amine M’Charrak, Beren Millidge, and Thomas Lukasiewicz. 2024. Predictive Coding beyond Correlations. arXiv:2306.15479. Retrieved from <https://arxiv.org/abs/2306.15479>.
- [83] Tommaso Salvatori, Luca Pinchetti, Beren Millidge, Yuhang Song, Tianyi Bao, Rafal Bogacz, and Thomas Lukasiewicz. 2022. Learning on Arbitrary Graph Topologies via Predictive Coding. *Advances in Neural Information Processing Systems* 35 (Dec. 2022), 38232–38244. <https://doi.org/10.48550/arXiv.2201.13180>
- [84] Tommaso Salvatori, Yuhang Song, Yujian Hong, Lei Sha, Simon Frieder, Zhenghua Xu, Rafal Bogacz, and Thomas Lukasiewicz. 2021. Associative Memories via Predictive Coding. In *Advances in Neural Information Processing Systems*, Vol. 34. 3874–3886. <https://doi.org/doi/10.5555/3540261.3540557>
- [85] Tommaso Salvatori, Yuhang Song, Thomas Lukasiewicz, Rafal Bogacz, and Zhenghua Xu. 2021. Predictive Coding Can Do Exact Backpropagation on Convolutional and Recurrent Neural Networks. arXiv: arXiv:2103.03725. Retrieved from <https://arxiv.org/abs/2103.03725>.
- [86] Tommaso Salvatori, Yuhang Song, Zhenghua Xu, Thomas Lukasiewicz, and Rafal Bogacz. 2022. Reverse Differentiation via Predictive Coding. *Proceedings of the AAAI Conference on Artificial Intelligence* 36, 7 (June 2022), 8150–8158. <https://doi.org/10.1609/aaai.v36i7.20788>
- [87] Tommaso Salvatori, Yuhang Song, Yordan Yordanov, Beren Millidge, Lei Sha, Cornelius Emde, Zhenghua Xu, Rafal Bogacz, and Thomas Lukasiewicz. 2024. A Stable, Fast, and Fully Automatic Learning Algorithm for Predictive Coding Networks. In *The Twelfth International Conference on Learning Representations*. <https://openreview.net/forum?id=RyUvzda8GH>
- [88] Benjamin Scellier and Yoshua Bengio. 2017. Equilibrium Propagation: Bridging the Gap between Energy-Based Models and Backpropagation. *Frontiers in Computational Neuroscience* 11 (2017). <https://doi.org/10.3389/fncom.2017.00024>
- [89] Samuel S. Schoenholz, Justin Gilmer, Surya Ganguli, and Jascha Sohl-Dickstein. 2017. Deep Information Propagation. In *International Conference on Learning Representations*. <https://openreview.net/forum?id=H1W1UN9gg>
- [90] Martin Schrimpf, Idan Asher Blank, Greta Tuckute, Carina Kauf, Eghbal A. Hosseini, Nancy Kanwisher, Joshua B. Tenenbaum, and Evelina Fedorenko. 2021. The neural architecture of language: Integrative modeling converges on predictive processing. *Proceedings of the National Academy of Sciences* 118, 45 (Nov. 2021), e2105646118. <https://doi.org/10.1073/pnas.2105646118>
- [91] Cory Shain, Idan Asher Blank, Marten van Schijndel, William Schuler, and Evelina Fedorenko. 2020. fMRI reveals language-specific predictive coding during naturalistic sentence comprehension. *Neuropsychologia* 138 (Feb. 2020), 107307. <https://doi.org/10.1016/j.neuropsychologia.2019.107307>
- [92] Y. Song. 2021. *Predictive coding inspires effective alternatives to backpropagation*. Ph.D. Thesis. University of Oxford.
- [93] Yuhang Song, Thomas Lukasiewicz, Zhenghua Xu, and Rafal Bogacz. 2020. Can the Brain Do Backpropagation? — Exact Implementation of Backpropagation in Predictive Coding Networks. In *Advances in Neural Information Processing Systems*, Vol. 33. 22566–22579. <https://doi.org/doi/10.5555/3495724.3497616>
- [94] Yuhang Song, Beren Millidge, Tommaso Salvatori, Thomas Lukasiewicz, Zhenghua Xu, and Rafal Bogacz. 2024. Inferring neural activity before plasticity as a foundation for learning beyond backpropagation. *Nature Neuroscience* (Jan. 2024), 1–11. <https://doi.org/10.1038/s41593-023-01514-1>
- [95] Mufeng Tang, Helen Barron, and Rafal Bogacz. 2023. Sequential Memory with Temporal Predictive Coding. *Advances in neural information processing systems* 36 (2023), 44341–44355. <https://doi.org/10.5555/3666122.3668041>
- [96] Mufeng Tang, Tommaso Salvatori, Beren Millidge, Yuhang Song, Thomas Lukasiewicz, and Rafal Bogacz. 2023. Recurrent predictive coding models for associative memory employing covariance learning. *PLOS Computational Biology* 19, 4 (April 2023), e1010719. <https://doi.org/10.1371/journal.pcbi.1010719>
- [97] Tadashi Taniguchi, Shingo Murata, Masahiro Suzuki, Dimitri Ognibene, Pablo Lanillos, Emre Ugur, Lorenzo Jamone, Tomoaki Nakamura, Alejandra Ciria, Bruno Lara, and Giovanni Pezzulo. 2023. World models and predictive coding for cognitive and developmental robotics: frontiers and challenges. *Advanced Robotics* 37, 13 (July 2023), 780–806. <https://doi.org/10.1080/01691864.2023.2225232>
- [98] Jakub M. Tomczak. 2022. *Deep Generative Modeling* (1st ed. 2022 edition ed.). Springer, Cham, Switzerland.
- [99] Alexander Tschantz and Beren Millidge. 2023. infer-actively/pypc. Retrieved from <https://github.com/infer-actively/pypc>.
- [100] Alexander Tschantz, Beren Millidge, Anil K. Seth, and Christopher L. Buckley. 2023. Hybrid predictive coding: Inferring, fast and slow. *PLOS Computational Biology* 19, 8 (Aug. 2023), e1011280. <https://doi.org/10.1371/journal.pcbi.1011280>
- [101] Hao Wang and Dit-Yan Yeung. 2020. A Survey on Bayesian Deep Learning. *ACM Comput. Surv.* 53, 5 (Sept. 2020), 108:1–108:37. <https://doi.org/10.1145/3409383>
- [102] Lin Wang, Lotte Schoot, Trevor Brothers, Edward Alexander, Lena Warnke, Minjae Kim, Sheraz Khan, Matti Hämäläinen, and Gina R. Kuperberg. 2023. Predictive coding across the left fronto-temporal hierarchy during language comprehension. *Cerebral Cortex (New York, N.Y.: 1991)* 33, 8 (April 2023), 4478–4497. <https://doi.org/10.1093/cercor/bhac356>

- [103] Isaac Ronald Ward, Jack Joyner, Casey Lickfold, Yulan Guo, and Mohammed Bennamoun. 2022. A Practical Tutorial on Graph Neural Networks. *ACM Comput. Surv.* 54, 10s (Sept. 2022), 205:1–205:35. <https://doi.org/10.1145/3503043>
- [104] James C. R. Whittington and Rafal Bogacz. 2017. An Approximation of the Error Backpropagation Algorithm in a Predictive Coding Network with Local Hebbian Synaptic Plasticity. *Neural Computation* 29, 5 (May 2017), 1229–1262. https://doi.org/10.1162/NECO_a_00949
- [105] Xiaohui Xie and H. Sebastian Seung. 2003. Equivalence of backpropagation and contrastive Hebbian learning in a layered network. *Neural Computation* 15, 2 (Feb. 2003), 441–454. <https://doi.org/10.1162/08997660376252988>
- [106] Muchao Ye, Xiaojiang Peng, Weihao Gan, Wei Wu, and Yu Qiao. 2019. AnoPCN: Video Anomaly Detection via Deep Predictive Coding Network. In *Proceedings of the 27th ACM International Conference on Multimedia (MM '19)*. 1805–1813. <https://doi.org/10.1145/3343031.3350899>
- [107] Ya-xiang Yuan. 2015. Recent advances in trust region algorithms. *Mathematical Programming* 151, 1 (June 2015), 249–281. <https://doi.org/10.1007/s10107-015-0893-2>
- [108] Anthony Zador, Sean Escola, Blake Richards, Bence Ölveczky, Yoshua Bengio, Kwabena Boahen, Matthew Botvinick, Dmitri Chklovskii, Anne Churchland, Claudia Clopath, James DiCarlo, Surya Ganguli, Jeff Hawkins, Konrad Körding, Alexei Koulikov, Yann LeCun, Timothy Lillicrap, Adam Marblestone, Bruno Olshausen, Alexandre Pouget, Cristina Savin, Terrence Sejnowski, Eero Simoncelli, Sara Solla, David Sussillo, Andreas S. Tolias, and Doris Tsao. 2023. Catalyzing next-generation Artificial Intelligence through NeuroAI. *Nature Communications* 14, 1 (March 2023), 1597. <https://doi.org/10.1038/s41467-023-37180-x>
- [109] Sergey Zagoruyko and Nikos Komodakis. 2016. Wide Residual Networks. In *Proceedings of the British Machine Vision Conference 2016 (BMVC 2016)*, Richard C. Wilson, Edwin R. Hancock, and William A. P. Smith (Eds.). BMVA Press. <https://doi.org/10.5244/C.30.87>
- [110] Umais Zahid, Qinghai Guo, and Zafeirios Fountas. 2023. Predictive Coding as a Neuromorphic Alternative to Backpropagation: A Critical Evaluation. *Neural Computation* 35, 12 (Nov. 2023), 1881–1909. https://doi.org/10.1162/neco_a_01620
- [111] Umais Zahid, Qinghai Guo, and Zafeirios Fountas. 2024. Sample as you Infer: Predictive Coding with Langevin Dynamics. In *Forty-first International Conference on Machine Learning*. <https://openreview.net/forum?id=6VQXLUy4sQ>
- [112] Umais Zahid, Qinghai Guo, Karl Friston, and Zafeirios Fountas. 2023. Curvature-Sensitive Predictive Coding with Approximate Laplace Monte Carlo. arXiv: 2303.04976. Retrieved from <https://arxiv.org/abs/2303.04976>.

A Expectation Maximization and Variational Inference

This appendix extends the discussion in section 3. We first explain why calculating the likelihood is intractable. Then, we discuss the EM algorithm in mathematical detail. Finally, we discuss variational inference, both for the PCN of Rao & Ballard, and multi-layer PCNs. We derive the variational free energy for both the case of a delta function and a Gaussian variational distribution.

A.1 Expectation Maximization

Given a datapoint $\mathbf{x}^{(n)}$, we wish to find the maximum likelihood estimate of the parameters θ , defined as those which maximizes the probability of the observed data:

$$\begin{aligned}\hat{\theta} &= \operatorname{argmax}_{\theta} p(\mathbf{x}^{(n)}|\theta) \\ &= \operatorname{argmin}_{\theta} \underbrace{\left[-\ln p_{\theta}(\mathbf{x}^{(n)}) \right]}_{\text{NLL}(\theta)},\end{aligned}\tag{A.1}$$

where we defined $\text{NLL}(\theta)$ as the negative log-likelihood cf. (17). Many deep learning models increase their expressivity through *latent* (hidden) variables \mathbf{z} , low-dimensional compared to \mathbf{x} . The idea of such variables is that they capture information that is not directly observable in \mathbf{x} , and they have a simpler probability distribution by design [74]. Latent variable models underlie much of the power of modern deep learning methods, in particular generative models [31, 74].

The relation between observed and latent variables is described by the joint distribution $p_{\theta}(\mathbf{x}, \mathbf{z})$. This is also called a *generative model*, because by sampling from it one can generate synthetic data points in the input space \mathbf{x} . From this one can obtain $p_{\theta}(\mathbf{x})$ by marginalizing over \mathbf{z} ,

$$p_{\theta}(\mathbf{x}) = \int d\mathbf{z} p_{\theta}(\mathbf{x}, \mathbf{z}).\tag{A.2}$$

This integral is often intractable [74]. Indeed, for PC this is also the case, which can be observed by filling in $p_{\theta}(\mathbf{x}, \mathbf{z}) = \exp(-E_{\theta}(\mathbf{x}, \mathbf{z}))$, and with the energy of Rao & Ballard, cf. (26) one has

$$\begin{aligned}p_{\theta}(\mathbf{x}) &= \int d\mathbf{z} p(\mathbf{x}, \mathbf{z}) \\ &\propto \int d\mathbf{z} \exp\left(\frac{1}{2} \left(\frac{1}{\sigma_x^2} (\mathbf{x} - f(W\mathbf{z}))^2 + \frac{1}{\sigma_z^2} (\mathbf{z} - \mathbf{z}^p)^2 \right)\right).\end{aligned}\tag{A.3}$$

which is generally intractable due to the nonlinearity in the integrand. The same holds for the multi-layer network with (32), where the integral becomes even more complicated. Hence, we cannot just minimize $\text{NLL}(\theta)$ directly. For general generative models, this can be solved in different ways – commonly through MCMC methods, or variational inference [31]. *Expectation Maximization* (EM), presented in (18) and (19) can be seen as a special case of variational inference [7, 19]. Here, we shall motivate EM in detail, highlighting the different steps required to get to IL.

EM in general. First, introduce some distribution $q_{\phi}(\mathbf{z})$ over the latent variables. Given a datapoint $\mathbf{x}^{(n)}$, EM proceeds in two steps [19, 54]. (1) E-step: given \mathbf{x} and the current parameters θ , construct a new distribution $q_{\phi}(\mathbf{z})$ of latent variables, using the current posterior $p_{\theta}(\mathbf{z}|\mathbf{x})$. (2) M-step: re-estimate the parameter θ to be those with maximum

likelihood, assuming $q_\phi(\mathbf{z})$ found in the previous step is the true distribution of \mathbf{z} . In other words:

$$q_\phi(\mathbf{z}) = p_\theta(\mathbf{z}|\mathbf{x}) \quad \text{(E-step),} \quad (\text{A.4})$$

$$\hat{\theta} = \operatorname{argmax}_\theta \mathbb{E}_q[\ln p_\theta(\mathbf{x}, \mathbf{z})] \quad \text{(M-step).} \quad (\text{A.5})$$

Taking the k -means clustering algorithm as an example, these two steps correspond to assigning points to clusters, and defining clusters based on points, respectively [50]. This process works because one can show that each EM iteration decreases the true NLL, or at worst leaves it unchanged [19]. This can be shown by writing both steps as minimization of a single functional: the variational free energy.

EM with variational free energy. Define the *variational free energy* \mathcal{F} as follows:

$$\begin{aligned} \mathcal{F} &:= D_{\text{KL}}[q_\phi(\mathbf{z})||p_\theta(\mathbf{x}, \mathbf{z})] \\ &= D_{\text{KL}}[q_\phi(\mathbf{z})||p_\theta(\mathbf{z}|\mathbf{x})] - \ln p_\theta(\mathbf{x}) \end{aligned} \quad (\text{A.6})$$

(derived below, cf. section A.2.1). Since KL-divergences are always positive, one sees that $\mathcal{F} \geq -\ln p_\theta(\mathbf{x})$, i.e., \mathcal{F} is an *upper bound* on the NLL.¹⁶ In other words, if minimized with respect to θ , the NLL is also minimized. Similarly, it can be shown that the E-step can be written as minimization of this function [61]. Thus, one can write a new version of EM as follows:

$$q_\phi(\mathbf{z}) = \operatorname{argmin}_q \mathcal{F}(q, \theta) \quad \text{(E-step),} \quad (\text{A.7})$$

$$\hat{\theta} = \operatorname{argmin}_\theta \mathcal{F}(q, \theta) \quad \text{(M-step).} \quad (\text{A.8})$$

Below we demonstrate how different choices of q lead to different VFEs. For now, it can be taken simply as an intuitive justification for why the EM process minimizes the NLL as desired.

EM with MAP estimation. Using the result in [61] that EM will minimize the NLL, we return to the first formulation, (A.4) and (A.5). At first sight, the E-step still looks problematic, since evaluating the posterior $p_\theta(\mathbf{z}|\mathbf{x}) = p_\theta(\mathbf{x}, \mathbf{z})/p_\theta(\mathbf{x})$ requires calculating the marginal likelihood $p_\theta(\mathbf{x})$. This is analogous to computing the partition function in statistical physics, which is generally intractable. A solution is to set q to a delta function, $q_\phi(\mathbf{z}) = \delta(\mathbf{z} - \tilde{\mathbf{z}})$, in which case the posterior is simply described by its maximum value. Put differently, we simplify the evaluation of the posterior in the E-step by a *maximum a posteriori (MAP)* estimation of $p(\mathbf{z}|\mathbf{x})$. With a delta-distribution, the expectation of (A.5) also simplifies, and we have

$$\tilde{\mathbf{z}} = \operatorname{argmax}_z p_\theta(\mathbf{x}, \mathbf{z}) \quad \text{(E-step),} \quad (\text{A.9})$$

$$\hat{\theta} = \operatorname{argmax}_\theta p_\theta(\mathbf{x}, \tilde{\mathbf{z}}) \quad \text{(M-step).} \quad (\text{A.10})$$

With this choice, the parameters of $q_\phi(\mathbf{z})$ are $\phi = \tilde{\mathbf{z}}$. We discuss this in more detail below. Thus, we see having a model for $\ln p_\theta(\mathbf{x}, \mathbf{z})$ is sufficient for minimizing the (upper bound of) the NLL using EM. By choosing a form for $p_\theta(\mathbf{x}, \mathbf{z})$ (or E) one obtains different models, including PC.

EM with partial steps. Writing EM as a minimization of the VFE, it can be shown that minimizations in both steps need not be *complete*, but can also be *partial* [61]. Taking steps that decreases \mathcal{F} (i.e., in a gradient descent formulation) will

¹⁶One can equivalently write $-\mathcal{F} \leq \ln p_\theta(\mathbf{x})$, i.e. $-\mathcal{F}$ as a lower bound to $\ln p_\theta(\mathbf{x})$. The marginal log-likelihood is also called the *model evidence*, hence $-\mathcal{F}$ is also called the evidence lower bound, or *ELBO*[74].

also minimize the NLL. Algorithms with partial E and/or M steps are called *generalized EM* algorithms [7, 61]. Thus, we can write our process using a partial M-step:

$$\tilde{z} = \underset{z}{\operatorname{argmin}} E(\mathbf{x}, z) \quad \text{(E-step)} \quad (\text{A.11})$$

$$\Delta\theta \propto -\frac{dE}{d\theta} \quad \text{(partial M-step)} \quad (\text{A.12})$$

this is standard IL as presented in section 2. Alternatively, we could also make the E-step partial:

$$\Delta z \propto -\frac{dE}{dz} \quad \text{(partial E-step)}, \quad (\text{A.13})$$

$$\Delta\theta \propto -\frac{dE}{d\theta} \quad \text{(partial M-step)}, \quad (\text{A.14})$$

which is the basis for incremental IL.

A.2 Variational Inference

Variational inference provides a more general understanding for why EM minimizes the NLL. It also provides a connection to the more general theory of variational methods used in statistical physics and machine learning, for instance in variational autoencoders (VAEs). We briefly explain the general idea.

A.2.1 General Idea. Consider Bayes' rule for the posterior $p(z|\mathbf{x})$:

$$p_\theta(z|\mathbf{x}) = \frac{p_\theta(\mathbf{x}, z)}{p_\theta(\mathbf{x})}. \quad (\text{A.15})$$

Ideally, we would like to compute this posterior, but this requires computing the prior distribution $p_\theta(\mathbf{x})$, which is typically intractable. Instead, variational methods attempt to approximate the posterior distribution with a so-called *variational posterior* $q_\phi(z)$ parametrized by ϕ , such that the KL-divergence between q_ϕ and $p(z|\mathbf{x})$,

$$D_{\text{KL}}[q_\phi(z)||p_\theta(z|\mathbf{x})] = \int dz q_\phi(z) \ln \frac{q_\phi(z)}{p_\theta(z|\mathbf{x})}$$

is minimized. By Bayes' rule, this becomes

$$\begin{aligned} D_{\text{KL}}[q_\phi(z)||p_\theta(z|\mathbf{x})] &= \int dz q(z) \ln \frac{q_\phi(z)}{p_\theta(\mathbf{x}, z)} + \ln p_\theta(\mathbf{x}) \\ &= \underbrace{D[q_\phi(z)||p_\theta(\mathbf{x}, z)]}_{=\mathcal{F}} + \ln p_\theta(\mathbf{x}), \end{aligned}$$

where we have recognized variational free energy \mathcal{F} introduced above, which we can calculate for a given generative model and variational posterior. Furthermore, since the KL divergence is non-negative,

$$\mathcal{F} \geq D[q_\phi(z)||p_\theta(z|\mathbf{x})], \quad (\text{A.16})$$

since $\ln p_\theta(\mathbf{x}) \leq 0$. Thus, if we minimize \mathcal{F} with respect to ϕ , our function q will get closer to the true posterior: we are performing variational inference. In addition, we see that \mathcal{F} is a tractable upper bound to the NLL: minimizing \mathcal{F} thus minimizes the NLL.

In calculations, it is useful to decompose \mathcal{F} into two terms:

$$\mathcal{F} = \underbrace{\int dz q(z) \ln q(z)}_{H[q(z)] = H[q]} + \underbrace{\int dz q(z) E(x, z)}_{E_q} \quad (\text{A.17})$$

where we have substituted $E(x, z) = -\ln p_\theta(x, z)$. To make notation less cluttered, we leave out ϕ from here onwards. In this expression one can fill in a generative model and variational posterior, which we do below. First, we consider the general form of the VFE for L latent vectors, which is:

$$\begin{aligned} \mathcal{F} &= D_{\text{KL}}[q(\{z^\ell\}) || p_\theta(x, \{z^\ell\})]. \\ &\equiv \int \prod_{\ell=1}^L dz^\ell q(\{z^\ell\}) \ln \frac{q(\{z^\ell\})}{p_\theta(x, \{z^\ell\})} \\ &= \underbrace{\int \prod_{\ell=1}^L dz^\ell q(\bar{z}) \ln q(\bar{z})}_{H[\bar{q}]} - \underbrace{\int \prod_{\ell=1}^L dz^\ell q(\bar{z}) E(x, \bar{z})}_{E_q}, \end{aligned}$$

where we used $E(x, \{z^\ell\}) = -\ln p_\theta(x, \{z^\ell\})$ and introduced the notation $\bar{z} = \{z^\ell\}$ to make notation less cluttered. For the multi-layer case, it is often assumed q factorizes over the layers, i.e.,¹⁷

$$\bar{q} = q(\bar{z}) = \prod_{\ell=1}^L q(z^\ell), \quad (\text{A.18})$$

whereupon the entropy becomes

$$\begin{aligned} H[\bar{q}] &= \int \prod_{\ell=1}^L dz^\ell q(z^\ell) \sum_{k=1}^L \ln q(z^k) \\ &= \sum_k \int dz^k q(z^k) \ln q(z^k) \underbrace{\prod_{\ell \neq k} \int dz^\ell q(z^\ell)}_{=1} \\ &= \sum_\ell H[q(z^\ell)], \end{aligned} \quad (\text{A.19})$$

i.e., the entropy factorizes into a sum of the entropies of the individual layers. The second term $E_{\bar{q}}$ is somewhat more complicated in general, since the latent vectors in different layers z^ℓ may be coupled through E even though $q(\bar{z})$ factorizes. If one assumes a hierarchical structure of the generative model, cf. (27), one may write:

$$E = \sum_{\ell=1}^L E(z^\ell | z^{\ell+1}) \quad (\text{A.20})$$

¹⁷This does not correspond to any realistic network architecture, since it effectively assumes that $q(z^\ell | z^{\ell-1}) = q(z^\ell)$, i.e., that the individual layers are completely independent. As a variational ansatz however, it is not unreasonable, at least in certain cases. In FNNs at large width for example, the central limit theorem implies that the layers are approximately Gaussian, so a Gaussian ansatz for each separate layer can still lead to good results.

where if E is given by (32) then $E(\mathbf{z}^\ell | \mathbf{z}^{\ell+1}) = \frac{1}{2} (\boldsymbol{\epsilon}^\ell)^T (\boldsymbol{\Sigma}^\ell)^{-1} \boldsymbol{\epsilon}^\ell + \ln \det \boldsymbol{\Sigma}^\ell$. This provides some simplification in $E_{\bar{q}}$:

$$\begin{aligned}
E_{\bar{q}} &= \int \prod_{\ell} d\mathbf{z}^\ell q(\mathbf{z}^\ell) \sum_k E(\mathbf{z}^k | \mathbf{z}^{k+1}) \\
&= \int d\mathbf{z}^1 q(\mathbf{z}^1) E(\mathbf{z}^0 | \mathbf{z}^1) \prod_{\ell \neq 1} \underbrace{\int d\mathbf{z}^\ell q(\mathbf{z}^\ell)}_{=1} \\
&\quad + \sum_k \int d\mathbf{z}^k d\mathbf{z}^{k+1} q(\mathbf{z}^k) q(\mathbf{z}^{k+1}) E(\mathbf{z}^k | \mathbf{z}^{k+1}) \prod_{\ell \neq k} \underbrace{\int d\mathbf{z}^\ell q(\mathbf{z}^\ell)}_{=1} \\
&\quad + \int d\mathbf{z}^L q(\mathbf{z}^L) E(\mathbf{z}^L | \mathbf{z}^p) \prod_{\ell \neq L} \underbrace{\int d\mathbf{z}^\ell q(\mathbf{z}^\ell)}_{=1} \\
&= \underbrace{\int d\mathbf{z}^1 q(\mathbf{z}^1) E(\mathbf{z}^0 | \mathbf{z}^1)}_{(1)} + \sum_{\ell} \underbrace{\int d\mathbf{z}^\ell d\mathbf{z}^{\ell+1} q(\mathbf{z}^\ell) q(\mathbf{z}^{\ell+1}) E(\mathbf{z}^\ell | \mathbf{z}^{\ell+1})}_{(2)} + \underbrace{\int d\mathbf{z}^L q(\mathbf{z}^L) E(\mathbf{z}^L | \mathbf{z}^p)}_{(3)}.
\end{aligned} \tag{A.21}$$

For L latent vectors assuming a hierarchical generative model and a factorized variational, this is the furthest one can simplify. Observe that (1) is identical to E_q in eq. (A.17), whereas (3) is slightly different, and (2) is more complex.

A.2.2 PCNs of Rao & Ballard: Delta-function variational. Recent work [60] presents an attempted derivation of PC using a delta function as the variational posterior, in which it is claimed that the VFE simply becomes equal to the energy. Unfortunately however, this derivation contains a basic mathematical error, which we explain below. An alternative derivation [10] also exists that instead uses a Gaussian as variational posterior, approximated using a Taylor series. Under certain assumptions, this leads to the claimed result. We review the both here and in the next subsection.

First, let us take an n_z -dimensional delta function as our variational posterior:

$$\delta^{(n_z)}(\mathbf{z} - \tilde{\mathbf{z}}) = \prod_{i=1}^{n_z} \delta(z_i - \tilde{z}_i). \tag{A.22}$$

For the differential entropy H_q in (A.17), this gives

$$\begin{aligned}
H_q &= \int d\mathbf{z} \delta^{(n_z)}(\mathbf{z} - \tilde{\mathbf{z}}) \ln \delta^{(n_z)}(\mathbf{z} - \tilde{\mathbf{z}}) \\
&= \int \prod_{i=1}^M dz_i \delta(z_i - \tilde{z}_i) \sum_{j=1}^M \ln \delta(z_j - \tilde{z}_j) \\
&= \sum_{j=1}^M \left(\int dz_j \delta(z_j - \tilde{z}_j) \ln \delta(z_j - \tilde{z}_j) \prod_{i \neq j} \underbrace{\int dz_i \delta(z_i - \tilde{z}_i)}_{=1} \right).
\end{aligned} \tag{A.23}$$

In [56] this is erroneously taken to be zero. We speculate that this is based on the intuition that the “entropy” of a deterministic function like $\delta(\mathbf{z})$ should vanish. In fact however, the differential entropy of the Dirac delta function is $-\infty$. If however one treats this as an additive constant to be dropped, then we have only the E_q term, so that

$$\mathcal{F} = E(\mathbf{x}, \tilde{\mathbf{z}}). \tag{A.24}$$

For this reason, [56] identify the VFE as simply the energy (or negative complete data log-likelihood) in this case.

A.2.3 PCNs of Rao & Ballard: Gaussian variational. Now we instead take q to be a multivariate Gaussian centered around \tilde{z} with covariance $\tilde{\Sigma}$, using a tilde to distinguish from the mean and covariance of the generative model. This generalizes the derivation in [10] to the multivariate case, i.e.,

$$q(z) = \frac{1}{\sqrt{(2\pi)^{n_z} \det \tilde{\Sigma}}} \exp\left(-\frac{1}{2}(z - \tilde{z})^T \tilde{\Sigma}^{-1}(z - \tilde{z})\right). \quad (\text{A.25})$$

For convenience, we label $a_i = z_i - \tilde{z}_i$, $A = \tilde{\Sigma}^{-1}$, and $Z = \sqrt{(2\pi)^{n_z} \det A^{-1}}$. Substituting this ansatz into (A.17), we have

$$\begin{aligned} H[q] &= \int dz q(z) \ln q(z) \\ &= -\frac{1}{2Z} \int da \left[\exp\left(-\frac{1}{2} \sum_{ij} a_i a_j A_{ij}\right) \sum_{nm} a_n a_m A_{nm} \right] - \ln Z \underbrace{\int dz q(z)}_{=1} \\ &= -\frac{1}{2Z} \sum_{nm} A_{nm} \underbrace{\int da \left[a_n a_m \exp\left(-\frac{1}{2} \sum_{ij} a_i a_j A_{ij}\right) \right]}_{\langle a_n a_m \rangle} - \ln Z, \end{aligned} \quad (\text{A.26})$$

where we have identified the simple Gaussian integral

$$\langle a_n a_m \rangle = \sqrt{\frac{(2\pi)^{n_z}}{\det A}} (A^{-1})_{mn}. \quad (\text{A.27})$$

Plugging this in and writing out the definition of Z , we thus obtain

$$\begin{aligned} H[q] &= -\frac{1}{2} \sum_n \delta_{nn} - \frac{1}{2} [n_z \ln(2\pi) + \ln \det \tilde{\Sigma}] \\ &= -\frac{1}{2} [n_z (\ln 2\pi + 1) + \ln \det \tilde{\Sigma}]. \end{aligned} \quad (\text{A.28})$$

Meanwhile for E_q , one obtains:

$$\begin{aligned} E_q &= \int dz q(z) E(x, z) \\ &= \frac{1}{2Z} \int dz \exp\left(-\frac{1}{2}(z - \tilde{z})^T \tilde{\Sigma}^{-1}(z - \tilde{z})\right) \left[(x - f(Wz))^T \Sigma_x (x - f(Wz)) \right. \\ &\quad \left. + (z - z^p)^T \Sigma_z (z - z^p) + D \right], \end{aligned} \quad (\text{A.29})$$

where $D = \frac{1}{2} ((n_x + n_z) \ln 2\pi + \ln [\det \Sigma_x \det \Sigma_z])$. This integral does not have a full closed-form solution due to the nonlinearity $f(Wz)$. In the absence of a specific expression for this function, there are several ways to proceed. If $f(Wz)$ admits a polynomial expansion in z , then all odd terms in the integrand vanish, and the resulting integrals of the form $\int dz z^n q(z)$ for $0 < n \in 2\mathbb{Z}_+$ are easily done. A more abstract way of proceeding would be to perform an Edgeworth expansion of $p(x, z)$, with some assumption about how the corresponding cumulants integrate against a Gaussian. Intermediate between these two is the approach taken by [10], which keeps E unspecified, and formally Taylor expands it to second order around the mean of the variational posterior $z = \tilde{z}$. However, this implicitly assumes that $f(Wz)$ does

not grow too fast in z (i.e., the polynomial expansion quickly truncates); otherwise, the fall-off of the Gaussian $q(z)$ is insufficiently fast for this approximation to apply for general functions. Furthermore, even in the special case where $\langle E(\mathbf{x}, z) \rangle_z = \tilde{z}$, there is no guarantee that expanding the energy around this point will yield a good approximation to the integral. If $E(\mathbf{x}, z)$ is sharply peaked at \tilde{z} however, then we may proceed as in [10]; to second order,

$$\begin{aligned} E(\mathbf{x}, z) &\approx E(\mathbf{x}, \tilde{z}) + \nabla_z E(\mathbf{x}, \tilde{z}) + \frac{1}{2} (z - \tilde{z})^T \nabla \nabla_z E(\mathbf{x}, \tilde{z}) (z - \tilde{z}) \\ &= E(\mathbf{x}, \tilde{z}) + \sum_i \frac{\partial E(\mathbf{x}, \tilde{z})}{\partial z_i} (z_i - \tilde{z}_i) + \frac{1}{2} \sum_{ij} \frac{\partial^2 E(\mathbf{x}, \tilde{z})}{\partial z_i \partial z_j} (z_i - \tilde{z}_i) (z_j - \tilde{z}_j). \end{aligned} \quad (\text{A.30})$$

We define $H = \nabla \nabla_z E(\mathbf{x}, \tilde{z})$ for the Hessian (the matrix of second order derivatives). This gives

$$\begin{aligned} E_q &= \int dz q(z) E(\mathbf{x}, z) \\ &\approx E(\mathbf{x}, \tilde{z}) \underbrace{\int dz q(z)}_{=1} + \sum_i \frac{\partial E(\mathbf{x}, \tilde{z})}{\partial z_i} \underbrace{\int dz q(z) (z_i - \tilde{z}_i)}_{=0} \\ &\quad + \frac{1}{2} \sum_{ij} \frac{\partial^2 E(\mathbf{x}, \tilde{z})}{\partial z_i \partial z_j} \int dz q(z) (z_i - \tilde{z}_i) (z_j - \tilde{z}_j), \end{aligned} \quad (\text{A.31})$$

where the second term vanishes since the integrand is odd. Defining the shorthand notation $z_j - \tilde{z}_j =: a_j$, the remaining integral is

$$\begin{aligned} \int dz q(z) (z_i - \tilde{z}_i) (z_j - \tilde{z}_j) &= Z^{-1} \int da \exp\left(-\frac{1}{2} \sum_{kl} a_k a_l A_{kl}\right) a_i a_j \\ &= Z^{-1} \sqrt{\frac{(2\pi)^{n_z}}{\det A}} (A^{-1})_{ij} = (A^{-1})_{ij} = \tilde{\Sigma}_{ij}, \end{aligned} \quad (\text{A.32})$$

and therefore

$$E_q \approx E(\mathbf{x}, \tilde{z}) + \frac{1}{2} \sum_{ij} H_{ij} \tilde{\Sigma}_{ij}. \quad (\text{A.33})$$

Collecting results, the variational free energy \mathcal{F} is then

$$\mathcal{F} = E(\mathbf{x}, \tilde{z}) + \frac{1}{2} \sum_{ij} H_{ij} \tilde{\Sigma}_{ij} - \frac{1}{2} \ln \det \tilde{\Sigma} - \frac{1}{2} n_z (\ln 2\pi + 1). \quad (\text{A.34})$$

Thus, in contrast to the approach via a delta function above, a Gaussian ansatz leads to a term for the covariance of the variational posterior, as well as higher-order derivatives of the energy function. Applying EM would then require an additional part of the E-step for $\tilde{\Sigma}$. However, minimizing \mathcal{F} with respect to $\tilde{\Sigma}$ yields

$$\frac{\partial \mathcal{F}}{\partial \Sigma_{ij}} = \frac{1}{2} H_{ij} - \frac{1}{2} (\tilde{\Sigma}^{-1})_{ij}, \quad (\text{A.35})$$

where we used the identity $\frac{\partial \ln \det A}{\partial A_{ij}} = (A^{-1})_{ji}$, which follows from Jacobi's formula, and symmetry of the covariance matrix. Thus, \mathcal{F} is optimized when:

$$\tilde{\Sigma}_{ij} = (H^{-1})_{ij}, \quad (\text{A.36})$$

for all i, j . This gives

$$\begin{aligned}\mathcal{F} &= E(\mathbf{x}, \bar{\mathbf{z}}) + \frac{1}{2} \underbrace{\sum_{ij} H_{ij}(H^{-1})_{ij}}_{=n_z} - \frac{1}{2} \ln \det H^{-1} - \frac{1}{2} n_z (\ln 2\pi + 1) \\ &= E(\mathbf{x}, \bar{\mathbf{z}}) - \frac{1}{2} \ln \det H^{-1} - \frac{1}{2} n_z \ln 2\pi\end{aligned}\tag{A.37}$$

where we used the symmetry of the Hessian. This is the multivariate counterpart to eq. (17) in [10]. In sum, under a second order Taylor approximation of E , the optimal covariance of the variational is equal to the Hessian of E . Interestingly, including this term was shown to have practical consequences in [112] training generative PCNs, with substantially improved sample qualities and log-likelihoods as a result. Hence, further studying the inclusion of higher-order terms in the minimization objective could potentially be an interesting avenue for further work. However, as noted by [112], such efforts need to balance potential increases in performance with increased computation. Moreover, better variational ansätze may encounter other practical issues, cf. [49, 50].

B Complementary Proofs and Miscellaneous

B.1 Backpropagation

We derive (5) and (6) from (4) and (1) in section 2.1.2. Observe that with the chain rule, (4) can be written as:

$$\begin{aligned}\delta_i^\ell &= \sum_j \frac{\partial \mathcal{L}}{\partial a_j^{\ell+1}} \frac{\partial a_j^{\ell+1}}{\partial a_i^\ell} \\ &= \sum_j \delta_j^{\ell+1} f' \left(\sum_k w_{jk}^\ell a_k^\ell \right) w_{ji}^\ell\end{aligned}\tag{A.38}$$

I.e. the error in layer ℓ can be expressed recursively using the error in the next layer, $\ell + 1$. Then, observe that the derivative with respect to weights can be expressed using this error:

$$\frac{\partial \mathcal{L}}{\partial w_{ij}^\ell} = \sum_k \frac{\partial \mathcal{L}}{\partial a_k^{\ell+1}} \frac{\partial a_k^{\ell+1}}{\partial w_{ij}^\ell} = \delta_i^{\ell+1} f' \left(\sum_n w_{in}^\ell a_n^\ell \right) a_j^\ell,\tag{A.39}$$

which using matrix notation gives the results in the main text.

B.2 Equivalence of FNNs and Discriminative PCNs During Testing

This appendix reproduces the proof in [92, 104] that inference (testing) in FNNs and discriminative PCNs is equivalent, cf. section 2.2.4 in the main text. During testing, clamp $\mathbf{a}^0 = \mathbf{x}^{(n)}$. We want to find

$$\hat{\mathbf{a}}^\ell = \underset{\mathbf{a}^\ell}{\operatorname{argmin}} E(\mathbf{a}, \mathbf{w})$$

for $\ell = 1, \dots, L$. The inferred value of the last layer \mathbf{a}^L is identified as the output $\hat{\mathbf{y}}$. Write the energy as:

$$E(\mathbf{a}, \mathbf{w}) = \frac{1}{2} \sum_{\ell=1}^L (\epsilon^\ell)^2 = \frac{1}{2} \left((\epsilon^L)^2 + (\epsilon^{L-1})^2 + \sum_{\ell=1}^{L-2} (\epsilon^\ell)^2 \right)\tag{A.40}$$

and note that $\epsilon^\ell = \mathbf{a}^\ell - f(\mathbf{w}^{\ell-1} \mathbf{a}^{\ell-1})$. To find the minimum, take the derivative w.r.t. \mathbf{a}^ℓ and set to zero, for all $\ell = 1, \dots, L$. First for $\ell = L$:

$$\frac{\partial E}{\partial \mathbf{a}^L} = \epsilon^L = \mathbf{a}^L - f(\mathbf{w}^{L-1} \mathbf{a}^{L-1}) = 0 \iff \mathbf{a}^L = f(\mathbf{w}^{L-1} \mathbf{a}^{L-1}).\tag{A.41}$$

For $\ell = L - 1$:

$$\frac{\partial E}{\partial \mathbf{a}^{L-1}} = \epsilon^L \frac{\partial \epsilon^L}{\partial \mathbf{a}^{L-1}} + \epsilon^{L-1} = 0.\tag{A.42}$$

Now from (A.41) we know that $\epsilon^L = 0$, and hence we have

$$\epsilon^{L-1} = 0 \iff \mathbf{a}^{L-1} = f(\mathbf{w}^{L-2} \mathbf{a}^{L-2}).\tag{A.43}$$

Continuing this argument for decreasing ℓ until $\ell = 0$ we obtain

$$\epsilon^1 = 0 \iff \mathbf{a}^1 = f(\mathbf{w}^0 \mathbf{a}^0).\tag{A.44}$$

Thus we have found that for $\ell = L, \dots, 1$,

$$\mathbf{a}^\ell = f(\mathbf{w}^{\ell-1} \mathbf{a}^{\ell-1}),\tag{A.45}$$

so with $\mathbf{a}^0 = \mathbf{x}^{(n)}$ and $\mathbf{a}^L = \hat{\mathbf{y}}$ we obtain exactly the relations for a FNN, cf. (1).

B.3 Structure in PCNs

Here, we briefly expand on the discussion in section 2.3.3. What precisely defines the *structure* of a PCN? PCNs adds error nodes through (8) on top of activity nodes; but to get connections between layers like in FNNs, one should also include predictions, (7). However, illustrations like fig. 5 also include feedback connections, a key aspect of PCNs – hence they could additionally be included under structure. Mathematically, one way of defining these connections is by the activity rule (10). However, this equation is derived from the minimum of the objective function, which also defines the learning algorithm. This illustrates how structure and learning algorithm are more difficult to separate in PCNs.

This discussion explains why the term predictive coding in the literature sometimes appears to relate to a learning algorithm, and sometimes to different network architectures. Indeed, we have explained that it is in fact *both*. Nonetheless, some aspects of these algorithms are clearly ‘structural’ in nature: hence we keep using these terms when useful (as e.g. in fig. 2).

B.4 Z-IL pseudocode

Cf. section 4.1 in the main text. Note that to write down Z-IL most simply we here use notation that contradicts other sections. We use $\mu^\ell = f(\mathbf{w}^{\ell+1} \mathbf{a}^{\ell+1})$, with data $\mathbf{x}^{(n)}$ clamped to \mathbf{a}^L to and $\mathbf{y}^{(n)}$ to \mathbf{a}^0 .

Algorithm 4 Learning $\{\mathbf{x}^{(n)}, \mathbf{y}^{(n)}\}$ with Z-IL, with updates equal to BP with MSE loss.

Require: : $\mu = f(\mathbf{w}^{\ell+1} \mathbf{a}^{\ell+1})$ // Downward predictions
Require: : $\mathbf{a}^L = \mathbf{x}^{(n)}, \mathbf{a}^0 = \mathbf{y}^{(n)}$ // Clamp data
Require: : $\mathbf{a}^\ell(0) = \mu^\ell(0)$ for $\ell = 1, \dots, L - 1$ // Feedforward-pass initialization
Require: : $\gamma = 1$
1: **for** $t = 0$ to L **do** // Note: $T = L$
2: **for** each ℓ **do**
3: $\mathbf{a}^\ell(t + 1) = \mathbf{a}^\ell(t) - \gamma \frac{\partial E}{\partial \mathbf{a}^\ell}$
4: $\mathbf{w}^{\ell=t}(t + 1) = \mathbf{w}^{\ell=t}(t) - \alpha \frac{\partial E}{\partial \mathbf{w}^{\ell=t}}$ // Note: $\ell = t$
5: **end for**
6: **end for**

C Computational Complexity

Here, we compare the time complexity of BP and IL. The practical computation time of these algorithms consists of (1) the complexity of one weight update, and (2) the number of weight updates until convergence, but the latter cannot be computed in general, since it depends on factors such as the dataset and optimizer used. However, (1) is tractable by considering the calculations in table 3. The most costly computations for each line are the matrix multiplications (including outer products). We can use the following:

- A matrix multiplication $(m \times n) \times (n \times p)$ has time complexity $O(mnp)$.
- The outer product of m -dim vector with n -dim vector is a matrix multiplication $(m \times 1) \times (1 \times n)$.

For example, this means that the matrix multiplication $\mathbf{w}^{\ell-1} \mathbf{a}^{\ell-1}$ has a complexity of $O(n^\ell n^{\ell+1})$. For convenience we define the complexity of the largest matrix multiplication as:

$$M = \max(\{n^\ell n^{\ell+1}\}_\ell). \quad (\text{A.46})$$

The results are shown in tables 7 for BP and 8 for IL and incremental IL. For both, the complexity without parallelization is shown, along with the results for parallelized layers ([PL]). It can be seen that with parallelized layers, standard IL is faster only if $T < L$, whereas incremental IL is faster by a factor L . For incremental IL, it should be noted that although the time complexity *per weight update* no longer scales with T , implementations so far suggest that, for a given epoch, one should still spend several inference iterations (i.e. E-steps) on a given datapoint/batch (in contrast with BP, which always performs a single forward and backward pass per batch). This means the *total* complexity would increase again with this factor. At the same time, it has been shown that low values T (e.g., $T = 3$ or 5 [5, 87]) appear to be sufficient, implying a substantial speed-up when L is large (which is common in modern deep learning). However, it is still unknown what values of T are appropriate in general.

Phase	TC/layer	Layers	BP	BP [PL]
Forward pass	M	$\ell : 0 \rightarrow L$	LM	LM
Backward pass	M	$\ell : L \rightarrow 1$	LM	LM
Weight update	M	$\forall \ell$	LM	M
Total			LM	LM

Table 7. **Time complexity (TC) of a single weight update for BP** in an FNN. TC is quantified with big-O notation where constant factors are ignored. [PL] refers to TC with parallelized layers, which has not yet been achieved in practice.

Phase	TC/layer/iteration	Time step, layers	IL	IL [PL]	i-IL	i-IL [PL]
Inference	M	$t : 0 \rightarrow T, \forall \ell$	TLM	TM	LM	M
Learning	M	$\forall \ell$	LM	M	LM	M
Total			TLM	TM	LM	M

Table 8. **Time complexity (TC) of a single weight update for IL and incremental IL (i-IL)** in a PCN. TC is quantified with big-O notation where constant factors are ignored. [PL] refers to TC with parallelized layers, which has not yet been achieved in practice.